R. & M. No. 2819
(12,222)
A.R.C. Technical Report

MINISTRY OF SUPPLY

AERONAUTICAL RESEARCH COUNCIL
REPORTS AND MEMORANDA

Theoretical Calculations of the Distribution of Aerodynamic Loading on a Delta Wing

By
H. C. GARNER, B.A.
of the Aerodynamics Division, N.P.L.

LONDON: HER MAJESTY'S STATIONERY OFFICE
1954
NINE SHILLINGS NET

Theoretical Calculations of the Distribution of Aerodynamic Loading on a Delta Wing

By

H. C. Garner, B.A.

of the Aerodynamics Division, N.P.L.

Reports and Memoranda No. 2819*

March, 1949

Summary.—The distribution of velocity potential difference has been calculated for a thin flat plate in the form of a delta wing at small incidence. The method introduces novel functions with 10 arbitrary constants to express the doublet distribution over the wing and a special numerical integration to evaluate the downwash at 10 chosen points on the surface. Three different forms of the doublet distribution (a), (b) and (c) are employed and lead to three independent solutions of the resulting simultaneous equations ; solution (c) is considered to be the most accurate.

The plan form selected for this investigation is that of a delta wing, of aspect ratio 3, shown in Fig. 1. One object of the laborious calculations is to form the first step towards a fundamental comparison with pressure distributions measured on a model of the wing in the National Physical Laboratory Duplex Wind Tunnel. Solution (c) has been compared with two solutions of the identical problem by vortex-lattice theory as given in R. & M. 2596[2], Tables 37 and 38 (Falkner, 1948), using respectively 6 and 8 simultaneous equations, *viz.*, solutions 33 and 34 of which the latter involves an auxiliary function P to allow for discontinuities at the median section.

Conclusions.—1. The values of $\partial C_L/\partial\alpha$ and positions of the aerodynamic centre relative to the trailing edge determined from solutions (a), (b) and (c) lie within 1 per cent and $\frac{1}{2}$ per cent respectively.

2. The pressure differences compare very well over most of the plan form, the discrepancies only becoming appreciable near the apex of the delta wing and the outboard trailing edge.

3. The calculated values of $\partial C_L/\partial\alpha$ in R. & M. 2596[2] are about 3 per cent (or perhaps 5 per cent) greater than those determined from the present method.

4. For a given C_L, the spanwise distribution of lift from vortex-lattice theory compares very well over most of the span but becomes too great towards the tips, as the conclusions of R. & M. 2225[3] (Jones, 1946) would suggest.

5. The position of the aerodynamic centre as given by solution 34 agrees better than solution 33 with the results of the present method near the median section, but both solutions give a notable difference in the distribution of loading at the median section, as shown in Fig. 6. This suggests that the mathematical form of the doublet distribution near the median section of a delta wing is of some importance (R. & M. 2721[1]).

6. The values of $\partial C_L/\partial\alpha$ and positions of the aerodynamic centre are in excellent agreement with experiment. Favourable comparisons between the theoretical and experimental pressure distributions are shown in Fig. 6.

Further Devolopments.—It is intended that the theoretical calculations should be extended to allow for wing thickness and further to provide an estimate of the pressure distribution in viscous incompressible flow. The calculated values would then be directly compared with the results from the pressure plotting experiments on the model of the delta wing.

It is suggested that a similar investigation should be undertaken to establish the aerodynamic characteristics associated with a swept trailing edge.

---

* Published with the permission of the Director, National Physical Laboratory.

1. *Introduction.*—It is generally recognised that there is a great need for a well-founded independent check on the existing theoretical methods of determining the pressure distribution on thin swept-back wings in inviscid, incompressible flow. A critical survey of the position has been presented in R. & M. 2721[1] (October, 1948); and the recommendations made in that report, in particular the second proposal, should be considered in the light of the results given in this report.

It is explained in R. & M. 2721[1], section 1, that the potential flow past a thin wing gives a distribution of lift per unit area

$$(p_b - p_a) = \rho V \frac{\partial}{\partial x} (\Phi_a - \Phi_b) , \qquad (1)$$

where the uniform undisturbed velocity V is in the direction Ox (Fig. 1) and $(\Phi_a - \Phi_b)$ is the difference between the velocity potentials on the upper and lower wing surfaces and is equivalent to the strength of the doublet distribution which defines the vortex sheet. $(\Phi_a - \Phi_b)$ is determined from the equations

$$w = \lim_{z_1 \to 0} \left(\frac{\partial \Phi}{\partial z_1}\right) = V \frac{\partial z\,(x,y)}{\partial x} , \qquad (2)$$

$$\Phi(x_1, y_1, z_1) = Vx + \frac{1}{4\pi} \iint_C (\Phi_a - \Phi_b) \frac{\partial}{\partial z_1} \left(\frac{1}{r}\right) dx\, dy , \qquad (3)$$

where $z\,(x,y)$ is the contour of the wing surface relative to the undisturbed stream, C is an area bounded by the leading edge of the wing and extending to infinity in the wake, and

$$r^2 = (x - x_1)^2 + (y - y_1)^2 + z_1^2 .$$

In the wake $(\Phi_a - \Phi_b)$ is a function of y only determined by its value at the trailing edge. A solution is obtained by assuming a general form for $(\Phi_a - \Phi_b)$ with arbitrary coefficients, by substituting $(\Phi_a - \Phi_b)$ in equation (3) to determine w in equation (2), by using the boundary condition expressed in equation (2) at a number of solving points to determine the arbitrary coefficients, and by evaluating $(p_b - p_a)$ from equation (1).

There are four questionable features, at least one of which appears in each practical method of solution considered in R. & M. 2721[1], section 2.2.

(*a*) The assumed form for $(\Phi_a - \Phi_b)$ adheres rigidly to the basic two-dimensional chordwise distributions.

(*b*) w is evaluated by splitting the continuous doublet distribution $(\Phi_a - \Phi_b)$ into a finite number of discrete vortices.

(*c*) w is inevitably infinite at virtually all points of a wing section at which the direction of the leading or trailing edge is discontinuous.

(*d*) The boundary condition (2) is satisfied at certain positions by a system of discrete vortices related two-dimensionally to $(p_b - p_a)$.

An independent check on the accuracy of such methods must steer clear of these possible sources of error. The theoretical calculation described in this report does achieve this at the expense of lengthy computation and therefore is unsuitable for general use.

The delta wing selected for this investigation has the plan form, shown in Fig. 1, with aspect ratio $A = 3$, a right-angled leading edge and cropped tips such that

$$\frac{\text{tip chord}}{\text{root chord}} = \frac{1}{7} .$$

Various suitable forms for the doublet distribution $(\Phi_a - \Phi_b)$ with 10 arbitrary coefficients have been chosen. A numerical method is used to evaluate the double integral for the downwash

$$w = \lim_{z_1 \to 0} \frac{\partial}{\partial z_1} \left[\frac{1}{4\pi} \iint_C (\Phi_a - \Phi_b) \frac{\partial}{\partial z_1} \left(\frac{1}{r} \right) dx\, dy \right] \quad \ldots \quad (4)$$

corresponding to each coefficient at the 10 points of the half plan-form, shown in Fig. 1. The investigation has been restricted to the uncambered wing in an inclined uniform stream. The boundary condition (2) then simplifies to

$$w = V\alpha , \quad \ldots \quad (5)$$

which provides 10 simultaneous linear equations to determine the unknown coefficients. By this process three different solutions have been obtained and the resulting pressure distributions from equation (1) are compared.

2. *General Form for Doublet Distribution.*—The problem is expressed in terms of rectangular co-ordinates (x,y,z) referred to the apex of the delta wing in the plane of symmetry, as shown in Fig. 1. The leading and trailing edges of the wing are denoted by

$$\left.\begin{array}{l} x = |y| \\ x = h \end{array}\right\}$$

respectively, and the semi-span is

$$s = \tfrac{6}{7}h .$$

The order of magnitude of the doublet distribution $(\Phi_a - \Phi_b)$ at the perimeter of the plan form is necessarily expressed by the conditions

$$\left.\begin{array}{ll} \dfrac{\Phi_a - \Phi_b}{hV} = O\left(\dfrac{x - |y|}{h}\right)^{1/2} & \text{near the leading edge} \\ \dfrac{\partial}{\partial x}\left(\dfrac{\Phi_a - \Phi_b}{V}\right) = 0 & \text{at the trailing edge} \\ \dfrac{\Phi_a - \Phi_b}{hV} = O\left(\dfrac{6}{7} - \dfrac{|y|}{h}\right)^{1/2} & \text{near the wing tip} \end{array}\right\} \quad \ldots \quad (6)$$

Two-dimensional conditions suggest that furthermore

$$\frac{\partial}{\partial x}\left(\frac{\Phi_a - \Phi_b}{V}\right) = O\left(\frac{h - x}{h}\right)^{1/2} \text{ near the trailing edge.} \quad \ldots \quad (7)$$

In order to satisfy (6), consider

$$\frac{\Phi_a - \Phi_b}{hV} = \left(\frac{x^2 - y^2}{hx}\right)^{1/2} \left[1 - \left(\frac{x^2 - y^2}{hx}\right) f(y)\right] .$$

Then $f(y)$ is chosen such that

$$\frac{\partial}{\partial x}\left(\frac{\Phi_a - \Phi_b}{V}\right) = \frac{1}{2}\left(\frac{hx}{x^2 - y^2}\right)^{1/2} \left(1 + \frac{y^2}{x^2}\right) \left[1 - \left(\frac{x^2 - y^2}{hx}\right) f(y)\right]$$

$$+ \left(\frac{x^2 - y^2}{hx}\right)^{1/2} \left[\left(-1 - \frac{y^2}{x^2}\right) f(y)\right] = 0 ,$$

when $x = h ,$

i.e., $$f(y) = \frac{h^2}{3(h^2 - y^2)} .$$

(59008) A 2

Then the three conditions of (6) will be satisfied by

$$\frac{\Phi_a - \Phi_b}{hV} = \left(\frac{x^2 - y^2}{hx}\right)^{1/2} \left[1 - \frac{h^2}{3(h^2 - y^2)}\left(\frac{x^2 - y^2}{hx}\right)\left\{1 - \left(\frac{7y}{6h}\right)^2\right\}^{1/2}\right]$$

$$= \Phi_0, \text{ say}$$

$$= \left(\frac{x'^2 - 4y'^2}{28x'}\right)^{1/2} \left[1 - \frac{196}{3(196 - y'^2)}\left(\frac{x'^2 - 4y'^2}{28x'}\right)\right]\left(\frac{144 - y'^2}{144}\right)^{1/2}, \quad (8)$$

where

$$\left.\begin{aligned} x' &= \frac{28x}{h} \\ y' &= \frac{14y}{h} = \frac{12y}{s} \end{aligned}\right\}.$$

Numerical values of Φ_0 are tabulated for integral and certain half values of x' and y' in Table 1. All the solutions are expressible in the general form

$$(\Phi_a - \Phi_b) = hV\Phi_0 \sum_p \sum_q A_{pq}(1 - X)^p (Y)^q, \quad \ldots \quad (9)$$

where X, Y denote $\frac{x}{h}$, $\frac{y}{s}$ respectively,

$$\left.\begin{aligned} &p \text{ takes values } 0, \tfrac{3}{2}, 2, 3, 4 \\ \text{and } &q \text{ takes values } 0, 2, 4, 6. \end{aligned}\right\}$$

Three particular forms of equation (9) have been used

$$\left.\begin{aligned} (a)\ \frac{\Phi_a - \Phi_b}{hV} &= \Phi_0 [\{A_1 + A_2(X - \tfrac{1}{2}X^2) + A_3(X - X^2 + \tfrac{1}{3}X^3) \\ &\quad + A_4(X - \tfrac{3}{2}X^2 + X^3 - \tfrac{1}{4}X^4)\} \\ &\quad + Y^2\{A_5 + A_6(X - \tfrac{1}{2}X^2) + A_7(X - X^2 + \tfrac{1}{3}X^3)\} \\ &\quad + Y^4\{A_8 + A_9(X - \tfrac{1}{2}X^2)\} + Y^6\{A_{10}\}]; \end{aligned}\right\} \quad (10a)$$

$$\left.\begin{aligned} (b)\ \frac{\Phi_a - \Phi_b}{hV} &= \Phi_0 \left[\left\{A_1\left(1 - \frac{4}{3\pi}(1 - X)^{3/2}\right) + A_2(X - \tfrac{1}{2}X^2)\right.\right. \\ &\quad \left. + A_3(X - X^2 + \tfrac{1}{3}X^3) + A_4(X - \tfrac{3}{2}X^2 + X^3 - \tfrac{1}{4}X^4)\right\} \\ &\quad + Y^2\left\{A_5\left(1 - \frac{4}{3\pi}(1 - X)^{3/2}\right) + A_6(X - \tfrac{1}{2}X^2)\right. \\ &\quad \left. + A_7(X - X^2 + \tfrac{1}{3}X^3)\right\} \\ &\quad + Y^4\left\{A_8\left(1 - \frac{4}{3\pi}(1 - X)^{3/2}\right) + A_9(X - \tfrac{1}{2}X^2)\right\} \\ &\quad \left. + Y^6\left\{A_{10}\left(1 - \frac{4}{3\pi}(1 - X)^{3/2}\right)\right\}\right]; \end{aligned}\right\} \quad (10b)$$

$$(c)\ \frac{\Phi_a - \Phi_b}{hV} = \Phi_0 \Big[\Big\{ A_1 - A_2 \cdot \frac{4}{3\pi}(1-X)^{3/2} + A_3(X - \tfrac{1}{2}X^2) + A_4(X - X^2 + \tfrac{1}{3}X^3) \Big\} + Y^2 \Big\{ A_5 - A_6 \cdot \frac{4}{3\pi}(1-X)^{3/2} + A_7(X - \tfrac{1}{2}X^2) \Big\} + Y^4 \Big\{ A_8 - A_9 \cdot \frac{4}{3\pi}(1-X)^{3/2} \Big\} + Y^6 \{A_{10}\} \Big], \quad \ldots \quad (10c)$$

where $X = \frac{x}{h}, \quad Y = \frac{y}{s}.$

(*a*) ignores the condition (7). (*b*) includes a somewhat rigid introduction of this condition. (*c*) is more flexible in that respect. The factor $4/3\pi$ is chosen in (*b*) because the chordwise distribution of pressure corresponding to

$$(\Phi_a - \Phi_b) = hV\Phi_0\left(1 - \frac{4}{3\pi}(1-X)^{3/2}\right)$$

at the median section $y = 0$ gives a ratio of circulation to the limiting value of

$$\left(\frac{h}{h-x}\right)^{1/2} \frac{\partial}{\partial x}\left(\frac{\Phi_a - \Phi_b}{V}\right)$$

at the trailing edge consistent with two-dimensional theory. It is noteworthy that the downwashes over the central half of the wing span due to the coefficient A_1 in (*b*) are remarkably uniform, as shown by the second column of Table 6B.

In general the lift coefficient is

$$C_L = \int_0^s \frac{4K\,dy}{VS},$$

where K, the circulation round a wing section, is equal to the value of $(\Phi_a - \Phi_b)$ at the trailing edge, $x = h$, and the surface area of the wing is

$$S = \tfrac{48}{49} h^2 .$$

Hence

$$C_L = \tfrac{7}{2} \int_0^1 \left(\frac{\Phi_a - \Phi_b}{hV}\right)_{x=h} dY . \quad \ldots \quad (11)$$

The pitching-moment coefficient about the trailing edge is given by

$$\tfrac{1}{2}\rho V^2 S\bar{c} C_m = 2\int_0^s \int_y^h (p_b - p_a)(h - x)\,dx\,dy ,$$

i.e.,

$$\tfrac{1}{2}\rho V^2 h^3 \cdot \tfrac{48}{49} \cdot \tfrac{4}{7} C_m = 2\int_0^s \int_y^h \rho V(h-x) \frac{\partial}{\partial x}(\Phi_a - \Phi_b)\,dx\,dy .$$

Therefore, on integration by parts,

$$\tfrac{96}{343} h^2 C_m = 2\int_0^s \int_y^h \left(\frac{\Phi_a - \Phi_b}{hV}\right) dx\,dy .$$

Hence

$$C_m = \tfrac{49}{8} \int_0^1 \int_{y/h}^1 \left(\frac{\Phi_a - \Phi_b}{hV}\right) dX\,dY . \quad \ldots \quad (12)$$

The chordwise centre of pressure along a wing section is at a distance p from the trailing edge given by

$$\frac{p}{h} = \frac{\int_y^h (p_b - p_a)(h - x)\,dx}{h\int_y^h (p_b - p_a)\,dx} = \frac{\int_{y/h}^1 (\Phi_a - \Phi_b)\,dX}{(\Phi_a - \Phi_b)_{x=h}} . \quad \ldots \quad (13)$$

The hinge of the elevon is taken at a distance 0·85 chord from the leading edge of the wing. Therefore the hinge-moment coefficient is given by

$$\tfrac{1}{2}\rho V^2 S_f \bar{c}_f C_H = -\cos\beta \int_{y_1}^{y_0}\int_{x_h}^{h} (p_b - p_a)(x - x_h)\,dx\,dy ,$$

where

$$x_h = 0{\cdot}85h + 0{\cdot}15y,$$

$$\beta = \cos^{-1}\frac{1}{\sqrt{(1{\cdot}0225)}} = \cos^{-1} 0{\cdot}988936$$

is the inclination of the hinge line to the y-axis, and

$$y_1 < y < y_0$$

is the spanwise extent of the elevon. It is convenient to consider the distribution of hinge moment on an elevon of full span $0 < y < s$. Then

$$\tfrac{48}{343}(0{\cdot}15h)^2 C_H = -\cos\beta \int_0^s \left[0{\cdot}15(h - y)\frac{K}{hV} - \int_{x_h}^h \left(\frac{\Phi_a - \Phi_b}{hV}\right) dx\right] dy ;$$

and

$$C_H = \int_0^1 C_h\,dY, \quad \ldots \quad (14)$$

where

$$C_h = -269{\cdot}21\left[0{\cdot}15\left(1 - \frac{y}{h}\right)\frac{K}{hV} - \int_{X_h}^1 \left(\frac{\Phi_a - \Phi_b}{hV}\right) dX\right]$$

and

$$X_h = \frac{x_h}{h} = 0{\cdot}85 + 0{\cdot}15\frac{y}{h} = 0{\cdot}85 + 0{\cdot}0107143y' .$$

In order to calculate p/h from equation (13) and C_h from equation (14), it is necessary to evaluate the integrals

$$\int_Y^1 \Phi_0 P\,dX \quad \text{and} \quad \int_{X_h}^1 \Phi_0 P\,dX , \quad \ldots \quad (15)$$

where Φ_0 is defined in equation (8) and given in Table 1, and in accordance with the equations (10) P represents each of the five functions of $X = x/h$

$$1,\ (X - \tfrac{1}{2}X^2),\ (X - X^2 + \tfrac{1}{3}X^3),$$

$$(X - \tfrac{3}{2}X^2 + X^3 - \tfrac{1}{4}X^4) \text{ and } \frac{4}{3\pi}(1 - X)^{3/2} .$$

The resulting integrals (15) are tabulated for the required values of $y' = 12Y$ in Tables 2A and 2B respectively. It is convenient to write each equation (10) in the form

$$\frac{\Phi_a - \Phi_b}{hV} = \Phi_0\left[B_1P_1 + B_2P_2 + B_3P_3 + B_4P_4\right] \quad \ldots \quad (16)$$

where

$$B_1 = A_1 + A_5Y^2 + A_8Y^4 + A_{10}Y^6 ,$$
$$B_2 = A_2 + A_6Y^2 + A_9Y^4 ,$$
$$B_3 = A_3 + A_7Y^2 ,$$
$$B_4 = A_4 .$$

For the solution (a) corresponding to equation (10a),

$$P_1 = 1\,,$$
$$P_2 = X - \tfrac{1}{2}X^2\,,$$
$$P_3 = X - X^2 + \tfrac{1}{3}X^3\,,$$
$$P_4 = X - \tfrac{3}{2}X^2 + X^3 - \tfrac{1}{4}X^4\,;$$

and, for example, the position of the chordwise centre of pressure from equation (13) is at a distance p from the trailing edge given by

$$\frac{p}{h} = \frac{\int_{y/h}^{1} \Phi_0(B_1P_1 + B_2P_2 + B_3P_3 + B_4P_4)\,dX}{(\Phi_0)_{x=h}\,(B_1 + \tfrac{1}{2}B_2 + \tfrac{1}{3}B_3 + \tfrac{1}{4}B_4)} \quad \ldots \quad (17)$$

For the particular doublet distributions defined in equations (10), C_L and C_m are evaluated from equations (11) and (12) to give the following formulae:—

(*a*)
$$\left.\begin{aligned} C_L &= 1\cdot64333(A_1 + \tfrac{1}{2}A_2 + \tfrac{1}{3}A_3 + \tfrac{1}{4}A_4) + 0\cdot36034(A_5 + \tfrac{1}{2}A_6 + \tfrac{1}{3}A_7) \\ &\quad + 0\cdot16664(A_8 + \tfrac{1}{2}A_9) + 0\cdot09881(A_{10})\,; \\ C_m &= 1\cdot57519A_1 + 0\cdot66795A_2 + 0\cdot47968A_3 + 0\cdot37198A_4 \\ &\quad + 0\cdot23060A_5 + 0\cdot10634A_6 + 0\cdot07403A_7 \\ &\quad + 0\cdot08494A_8 + 0\cdot04028A_9 + 0\cdot04336A_{10}\,. \end{aligned}\right\} \quad \ldots \quad (18a)$$

(*b*)
$$\left.\begin{aligned} C_L &= 1\cdot64333(A_1 + \tfrac{1}{2}A_2 + \tfrac{1}{3}A_3 + \tfrac{1}{4}A_4) + 0\cdot36034(A_5 + \tfrac{1}{2}A_6 + \tfrac{1}{3}A_7) \\ &\quad + 0\cdot16664(A_8 + \tfrac{1}{2}A_9) + 0\cdot09881(A_{10})\,; \\ C_m &= 1\cdot43194A_1 + 0\cdot66795A_2 + 0\cdot47968A_3 + 0\cdot37198A_4 \\ &\quad + 0\cdot21828A_5 + 0\cdot10634A_6 + 0\cdot07403A_7 \\ &\quad + 0\cdot08174A_8 + 0\cdot04028A_9 + 0\cdot04208A_{10}\,. \end{aligned}\right\} \quad \ldots \quad (18b)$$

(*c*)
$$\left.\begin{aligned} C_L &= 1\cdot64333(A_1 + \tfrac{1}{2}A_3 + \tfrac{1}{3}A_4) + 0\cdot36034(A_5 + \tfrac{1}{2}A_7) \\ &\quad + 0\cdot16664(A_8) + 0\cdot09881(A_{10})\,; \\ C_m &= 1\cdot57519A_1 - 0\cdot14326A_2 + 0\cdot66795A_3 + 0\cdot47968A_4 \\ &\quad + 0\cdot23060A_5 - 0\cdot01233A_6 + 0\cdot10634A_7 \\ &\quad + 0\cdot08494A_8 - 0\cdot00320A_9 + 0\cdot04336A_{10}\,. \end{aligned}\right\} \quad \ldots \quad (18c)$$

The position of the aerodynamic centre is at a distance $\bar{p}$ from the trailing edge, where

$$\frac{\bar{p}}{h} = \frac{\bar{c}C_m}{hC_L} = \frac{4}{7}\frac{C_m}{C_L}\,. \quad \ldots \quad (19)$$

3. *Method of Evaluation of Downwash.*—From equation (4), the downwash at a point (x_1, y_1) due to a doublet distribution $(\Phi_a - \Phi_b)$ is

$$w = \lim_{z_1 \to 0} \frac{1}{4\pi} \iint_C (\Phi_a - \Phi_b) \frac{\partial^2}{\partial z_1^2}\left(\frac{1}{r}\right) dx\,dy\,, \quad \ldots \quad (20)$$

where C is an area defined by

$$\left.\begin{aligned} |y| \leqslant x &< \infty \\ -s \leqslant y &\leqslant s \end{aligned}\right\}$$

and $$r^2 = (x - x_1)^2 + (y - y_1)^2 + z_1^2\,.$$

In a region excluding the singularity (x_1, y_1), equation (20) becomes

$$w_0 = -\frac{1}{4\pi}\iint \frac{\Phi_a - \Phi_b}{r^3}\, dx\, dy .$$

Putting $\quad \dfrac{x}{h} = \dfrac{x'}{28}, \quad \dfrac{y}{h} = \dfrac{y'}{14}, \quad \dfrac{x_1}{h} = \dfrac{x_1'}{28}, \quad \dfrac{y_1}{h} = \dfrac{y_1'}{14},$

$$\frac{r^3}{h^3} = \left\{\frac{(x' - x_1')^2 + 4(y' - y_1')^2}{784}\right\}^{3/2} .$$

Therefore outside the singularity the double integral becomes

$$\frac{w_0}{V} = -\frac{14}{\pi}\iint_{C-R}\left(\frac{\Phi_a - \Phi_b}{hV}\right)\frac{dx'\, dy'}{\{(x' - x_1')^2 + 4(y' - y_1')^2\}^{3/2}} . \quad \ldots \quad (21)$$

The downwash is determined by splitting the area C into a small rectangle R surrounding (x_1, y_1) symmetrically and the remainder $(C - R)$, over which equation (21) can be evaluated by direct numerical integration. The contribution, w_1, to the complete downwash, w, in equation (20) from the area R is obtained as a linear function of the values of $\left(\dfrac{\Phi_a - \Phi_b}{hV}\right)$ at 25 points on and inside R, shown in Fig. 1. By expressing $\left(\dfrac{\Phi_a - \Phi_b}{hV}\right)$ in terms of these 25 values as a polynomial in powers of $(x' - x_1')$ and $(y' - y_1')$, the 25 corresponding factors are found to be independent of the position (x_1, y_1). It is apparent that from the point of view of accuracy in w_1, it is desirable to keep R as small as possible. But if R becomes too small, the evaluation of equation (21) over the area $(C - R)$ becomes difficult and w/V becomes the difference between two large quantities, both tending to infinity as the dimensions of R tend to zero. Consequently it has been necessary to establish the accuracy of the foregoing method of evaluation by varying the size and shape of R. The writer is satisfied that at each of the ten solving points, shown in Fig. 1, the values of w/V due to the basic doublet distribution Φ_0 in equation (8) are within $\pm\, 0{\cdot}05$ per cent. Moreover the method is of universal application, provided that (x_1, y_1) does not lie too close to the leading edge or tips of a wing and the required distribution of w/V is continuous. Although the process of calculation is laborious and requires very accurate computation, it is quite straightforward.

The rectangle R is chosen to be

$$\left.\begin{array}{l} |\xi| = |x' - x_1'| \leqslant 1 \\ |\eta| = |y' - y_1'| \leqslant 1 \end{array}\right\} \quad \ldots \quad (22)$$

Let $G(\xi, \eta)$ denote the value of $\left(\dfrac{\Phi_a - \Phi_b}{hV}\right)$ at $(x', y') \equiv (x_1' + \xi,\ y_1' + \eta)$.

The contribution w/V from the area $(C - R)$ in equation (21) is

$$\frac{w_0}{V} = -\frac{14}{\pi}\left[\int_{-12}^{y_1'-1} + \int_{y_1'+1}^{12}\left\{\int_{2y'}^{\infty} F(x', y')\, dx'\right\} dy' + \int_{y_1'-1}^{y_1'+1}\left\{\int_{2y'}^{x_1'-1} + \int_{x_1'+1}^{\infty} F(x', y')\, dx'\right\} dy'\right], \quad (23)$$

where $\quad F(x', y') = \left(\dfrac{\Phi_a - \Phi_b}{hV}\right)\Big/\{(x' - x_1')^2 + 4(y' - y_1')^2\}^{3/2}$

$$= \frac{G(\xi, \eta)}{(\xi^2 + 4\eta^2)^{3/2}} .$$

Consider first the integration with respect to x'. It is necessary to give separate treatment to each doublet distribution

$$\left(\frac{\Phi_a - \Phi_b}{hV}\right) = \Phi_0 P ,$$

defined in equation (15). The factors $(\xi^2 + 4\eta^2)^{-3/2}$ are tabulated in Table 3, as these are of general use in computing the integrand $F(x',y')$ for integral values of x'. Over most of the plan form evaluation of the integrals may be carried out by means of Simpson's rule, *e.g.*,

$$\int_{14}^{16} F(x')\, dx' = \frac{F(14) + 4F(15) + F(16)}{3} \quad \ldots \qquad (24)$$

It is necessary to make occasional use of the formula

$$\int_{25}^{28} F(x')\, dx' = \frac{1\cdot125F(25) + 3\cdot375F(26) + 3\cdot375F(27) + 1\cdot125F(28)}{3} \quad \ldots \qquad (25)$$

in order to complete an integration. Near the leading edge, $x' = 2y'$, $F(x',y')$ behaves as $O\sqrt{(x' - 2y')}$ and this is taken into account by the formulae

$$\left.\begin{aligned} \int_{2y'}^{2y'+2} F(x')\, dx' &= \frac{4\cdot52548F(2y' + 1) + 0\cdot8F(2y' + 2)}{3} \\ \int_{2y'}^{2y'+3} F(x')\, dx' &= \frac{4\cdot45384F(2y' + 1) + 2\cdot51948F(2y' + 2) + 1\cdot37143F(2y' + 3)}{3} \end{aligned}\right\} \quad \ldots \qquad (26)$$

Downstream of the trailing edge $\left(\frac{\Phi_a - \Phi_b}{hV}\right) = \frac{K}{hV}$ is independent of x', and the integral

$$\int_{28}^{\infty}\left(\frac{\Phi_a - \Phi_b}{hV}\right)\left\{(x' - x_1')^2 + 4(y' - y_1')^2\right\}^{-3/2} dx'$$

$$= \frac{K}{hV} \cdot \frac{1}{4(y' - y_1')^2}\left[\frac{(x' - x_1')}{\sqrt{\{(x' - x_1')^2 + 4(y' - y_1')^2\}}}\right]_{28}^{\infty} \quad \ldots \qquad (27)$$

where the factors

$$\frac{1}{4(y' - y_1')^2}\left\{1 - \frac{28 - x_1'}{\sqrt{\{(28 - x_1')^2 + 4(y' - y_1')^2\}}}\right\}$$

are given in Table 4.

Near the singularity the integrand $F(x',y')$ becomes large as $O(r^{-3})$, while $\left(\frac{\Phi_a - \Phi_b}{hV}\right)$ remains a well-behaved function of x' and y'. It is necessary to express the doublet distribution as $G(\xi)$, a polynomial in $\xi = x' - x_1'$ and to use a special method of evaluation. Consider

$$\int_{\xi_1}^{\xi_3} \frac{G(\xi)\, d\xi}{(\xi^2 + 4\eta^2)^{3/2}}$$

where $\xi_3 - \xi_2 = \xi_2 - \xi_1 = \delta$ and $G(\xi)$ is taken in the form

$$G(\xi_1)\,\frac{(\xi - \xi_2)(\xi - \xi_3)}{(\xi_1 - \xi_2)(\xi_1 - \xi_3)} + G(\xi_2)\,\frac{(\xi - \xi_3)(\xi - \xi_1)}{(\xi_2 - \xi_3)(\xi_2 - \xi_1)} + G(\xi_3)\,\frac{(\xi - \xi_1)(\xi - \xi_2)}{(\xi_3 - \xi_1)(\xi_3 - \xi_2)} \, .$$

The problem of numerical evaluation reduces to the three integrals

$$\left.\begin{aligned} I_2 &= \int_{\xi_1}^{\xi_3} \frac{\xi^2\, d\xi}{(\xi^2 + 4\eta^2)^{3/2}} = \left[\log_e\{\xi + \sqrt{(\xi^2 + 4\eta^2)}\} - \frac{\xi}{\sqrt{(\xi^2 + 4\eta^2)}}\right]_{\xi_1}^{\xi_3} \\ I_1 &= \int_{\xi_1}^{\xi_3} \frac{\xi d\xi}{(\xi^2 + 4\eta^2)^{3/2}} = \left[- \frac{1}{\sqrt{(\xi^2 + 4\eta^2)}}\right]_{\xi_1}^{\xi_3} \\ I_0 &= \int_{\xi_1}^{\xi_3} \frac{d\xi}{(\xi^2 + 4\eta^2)^{3/2}} = \left[\frac{\xi}{4\eta^2\sqrt{(\xi^2 + 4\eta^2)}}\right]_{\xi_1}^{\xi_3} \end{aligned}\right\} \quad \ldots \quad (28)$$

Hence

$$\begin{aligned} \int_{\xi_1}^{\xi_3} \frac{G(\xi)\, d\xi}{(\xi^2 + 4\eta^2)^{3/2}} &= \frac{1}{2\delta^2}\Big[G(\xi_1)\{I_2 - (\xi_2 + \xi_3)I_1 + \xi_2\xi_3 I_0\} \\ &\quad + G(\xi_2)\{- 2I_2 + 2(\xi_3 + \xi_1)I_1 - 2\xi_3\xi_1 I_0\} \\ &\quad + G(\xi_3)\{I_2 - (\xi_1 + \xi_2)I_1 + \xi_1\xi_2 I_0\}\Big] \\ &= \sum_1^3 C_n G(\xi_n), \quad \ldots \quad (29) \end{aligned}$$

where the factors C_n depend on ξ_1, ξ_2, ξ_3 and η. When $|\eta| \leqslant 1$, the formula (29) is used for the range $1 \leqslant |\xi| \leqslant 5$. When $1 \leqslant |\eta| \leqslant 3$, it is used for $|\xi| \leqslant 3$. The factors, shown in Table 5, are independent of (x_1', y_1').

The formulae (24), (25), (26), (27) and (29) are sufficient to determine the integrals with respect to x'. Let

$$\left.\begin{aligned} Y_1(y') &= \int_{2y'}^{\infty} F(x',y')\, dx' \\ Y_2(\eta) = Y_2(y' - y_1') &= \int_{2y'}^{x_1'-1} F(x',y' - y_1')\, dx' \\ Y_3(\eta) = Y_3(y' - y_1') &= \int_{x_1'+1}^{\infty} F(x',y' - y_1')\, dx' \end{aligned}\right\} \quad \ldots \quad (30)$$

Then the contribution to w/V from $(C - R)$ in equation (23) becomes

$$\begin{aligned} \frac{w_0}{V} = -\frac{14}{\pi}\Big[\int_{-12}^{y_1'-1} Y_1(y')\, dy' + \int_{y_1'+1}^{12} Y_1(y')\, dy' \\ + \int_{-1}^{+1}\{Y_2(\eta) + Y_3(\eta)\}\, d\eta\Big]. \quad \ldots \quad (31) \end{aligned}$$

The spanwise integrations must be carried out for series of doublet distributions differing in respect of factors dependent on y' only. From equations (9) and (10) it is seen that the general form to be considered is

$$\left(\frac{\Phi_a - \Phi_b}{hV}\right) = \Phi_0 P \left(\frac{y'}{12}\right)^q$$

where $q = 0, 2, 4, 6$. Thus the integrands (30) require various factors $(y'/12)^q$ and the integrals (31) have to be evaluated in each case.

$Y_1(y')$ is evaluated for integral values of y' and is integrated by Simpson's rule, *e.g.*, equation (24), except near the tips $y' = \pm 12$, where the formulae (26) apply, and near the singularity, where $Y_1(y')$ behaves as $O\left(\frac{1}{(y'-y_1')^2}\right)$. In the regions $3 \leqslant |y' - y_1'| \leqslant 5$, $1 \leqslant |y' - y_1'| \leqslant 3$, $Y_1(y')$ is expressed in the form

$$\frac{a + b(y' - y_1')^2 + c(y' - y_1')^4}{(y' - y_1')^2} ;$$

and the resulting formulae

$$\left.\begin{aligned} \int_{y_1'-5}^{y_1'-3} Y(y')\, dy' &= \frac{245Y_1(y_1'-5) + 1024Y_1(y_1'-4) + 243Y_1(y_1'-3)}{756} \\ \int_{y_1'-3}^{y_1'-1} Y(y')\, dy' &= \frac{27Y_1(y_1'-3) + 128Y_1(y_1'-2) + 25Y_1(y_1'-1)}{90} \end{aligned}\right\} \quad .. \quad (32)$$

are used to complete the integrations of Y_1. An exception arises in the particular instance $y_1' = 10$, when by writing

$$Y_1(y') = \frac{\sqrt{(12-y')}}{(y'-10)^2}\left\{Y_1(11)(23-2y') - Y_1(11\tfrac{1}{2})\,.\,\frac{9\sqrt{2}}{2}(y'-11)\right\},$$

the following formula is deduced :

$$\int_{11}^{12} Y_1(y')\, dy' = 0{\cdot}144522Y_1(11) + 0{\cdot}739023Y_1(11\tfrac{1}{2}) \,. \quad .. \quad .. \quad .. \quad .. \quad (33)$$

To calculate the remaining integral of equation (31),

$$\int_{-1}^{1} \{Y_2(\eta) + Y_3(\eta)\}\, d\eta ,$$

Y_2 and Y_3 are evaluated for $y' - y_1' = \eta = -1, -\frac{1}{2}, 0, \frac{1}{2}, 1$. Consider first the integrand, when the doublet strength is independent of x'. On writing $F = (\xi^2 + 4\eta^2)^{-3/2}$ in equation (30) it follows from equation (28) that

$$\begin{aligned} \int_{\xi}^{\infty} \frac{d\xi}{(\xi^2 + 4\eta^2)^{3/2}} &= \left[\frac{\xi}{4\eta^2\sqrt{(\xi^2 + 4\eta^2)}}\right]_{\xi}^{\infty} \\ &= \frac{1}{\sqrt{(\xi^2+4\eta^2)}\{\xi + \sqrt{(\xi^2+4\eta^2)}\}} , \end{aligned}$$

where, for the special rectangle R in equation (22), $\xi = 1$.

Y_2 and Y_3 are therefore considered in the general form

$$Y_2(\eta) = \frac{a_0 + a_1\eta + a_2\eta^2}{\sqrt{(\xi^2+4\eta^2)}\{\xi + \sqrt{(\xi^2+4\eta^2)}\}} .$$

By equating values at the positions $\eta = 0, \frac{1}{2}, 1$, it follows that

$$\left.\begin{aligned} a_0 &= 2\xi^2 Y_2(0) \\ a_1 &= -6\xi^2 Y_2(0) + 4\sqrt{(\xi^2+1)}\{\xi + \sqrt{(\xi^2+1)}\}Y_2(\tfrac{1}{2}) \\ &\quad - \sqrt{(\xi^2+4)}\{\xi + \sqrt{(\xi^2+4)}\}Y_2(1) \\ a_2 &= 4\xi^2 Y_2(0) - 4\sqrt{(\xi^2+1)}\{\xi + \sqrt{(\xi^2+1)}\}Y_2(\tfrac{1}{2}) \\ &\quad + 2\sqrt{(\xi^2+4)}\{\xi + \sqrt{(\xi^2+4)}\}Y_2(1) \end{aligned}\right\} \quad .. \quad .. \quad .. \quad (34)$$

Then

$$\int_0^1 Y_2(\eta)\,d\eta = \int_0^1 \frac{a_0 + a_1\eta + a_2\eta^2}{\sqrt{(\xi^2 + 4\eta^2)}\{\xi + \sqrt{(\xi^2 + 4\eta^2)}\}}\,d\eta$$

$$= a_0\left(\frac{\sqrt{(\xi^2+4)}}{4\xi} - \frac{1}{4}\right) + \frac{a_1}{4}\log_e \frac{\sqrt{(\xi^2+4)}+\xi}{2\xi}$$

$$+ a_2\left(\frac{1}{4} - \frac{\xi}{8}\log_e \frac{\sqrt{(\xi^2+4)}+2}{\xi}\right). \quad \ldots \quad (35)$$

By substituting $\xi = 1$ in equations (34) and (35),

$$\int_0^1 Y_2(\eta)\,d\eta = 0{\cdot}309017a_0 + 0{\cdot}120303a_1 + 0{\cdot}069546a_2\,,$$

where

$$a_0 = 2Y_2(0)$$

$$a_1 = -6Y_2(0) + 13{\cdot}65685Y_2(\tfrac{1}{2}) - 7{\cdot}23607Y_2(1)$$

$$a_2 = 4Y_2(0) - 13{\cdot}65685Y_2(\tfrac{1}{2}) + 14{\cdot}47214Y_2(1)\,.$$

Thus

$$\int_{-1}^1 Y_2(\eta)\,d\eta = 0{\cdot}348797Y_2(0) + 0{\cdot}693186\{Y_2(-\tfrac{1}{2}) + Y_2(\tfrac{1}{2})\}$$

$$+ 0{\cdot}135953\{Y_2(-1) + Y_2(1)\}\,, \quad \ldots \quad (36)$$

and an identical formula is used for

$$\int_{-1}^1 Y_3(\eta)\,d\eta\,.$$

By means of the formulae (32), (33) and (36), equation (31) may be evaluated to determine the contribution w_0/V from the area $(C - R)$ for each equation (10) for $\left(\frac{\Phi_a - \Phi_b}{hV}\right)$ in terms of the coefficients $A_1, A_2, \ldots A_{10}$.

Now consider the treatment of equation (20) in a region containing the singularity. The contribution to w/V from the area R, defined in equation (22), is

$$\frac{w_1}{V} = \lim_{z_1 \to 0}\left[\frac{h}{4\pi}\int\!\!\int_R \left(\frac{\Phi_a - \Phi_b}{hV}\right)\frac{\partial^2}{\partial z_1^2}\left(\frac{1}{r}\right)dx\,dy\right.$$

$$= \lim_{z_1 \to 0}\left[\frac{h}{4\pi}\int\!\!\int_R \left(\frac{\Phi_a - \Phi_b}{hV}\right)\left\{-\frac{\partial^2}{\partial x^2}\left(\frac{1}{r}\right) - \frac{\partial^2}{\partial y^2}\left(\frac{1}{r}\right)\right\}dx\,dy\right], \quad \ldots \quad (37)$$

which, by the use of Stoke's theorem*, becomes

---

* In vector notation, $\int\!\!\int_R \left(\frac{\partial A_y}{\partial x} - \frac{\partial A_x}{\partial y}\right)dx\,dy = \int\!\!\int_R \operatorname{curl} \underset{\sim}{A}\,.\,d\underset{\sim}{S}$

$$= \oint \underset{\sim}{A}\,.\,d\underset{\sim}{s}$$

$$= \oint (A_x\,dx + A_y\,dy)\,,$$

taken round R in a clockwise direction. The equivalence of equations (37) and (38) is apparent by substituting

$$\left.\begin{aligned} A_x &= \left(\frac{\Phi_a - \Phi_b}{hV}\right)\frac{\partial}{\partial y}\left(\frac{1}{r}\right) \\ A_y &= -\left(\frac{\Phi_a - \Phi_b}{hV}\right)\frac{\partial}{\partial x}\left(\frac{1}{r}\right)\end{aligned}\right\}.$$

$$\frac{h}{4\pi}\left[\int_{x_1-\frac{1}{28}h}^{x_1+\frac{1}{28}h}\left(\frac{\Phi_a-\Phi_b}{hV}\right)\frac{\partial}{\partial y}\left(\frac{1}{r}\right)dx\right]_{y=y_1+\frac{1}{14}h}^{y=y_1-\frac{1}{14}h} - \frac{h}{4\pi}\left[\int_{y_1-\frac{1}{14}h}^{y_1+\frac{1}{14}h}\left(\frac{\Phi_a-\Phi_b}{hV}\right)\frac{\partial}{\partial x}\left(\frac{1}{r}\right)dy\right]_{x=x_1-\frac{1}{28}h}^{x=x_1+\frac{1}{28}h}$$

$$+\frac{h}{4\pi}\int_R\int\left\{\frac{\partial}{\partial x}\left(\frac{\Phi_a-\Phi_b}{hV}\right)\frac{\partial}{\partial x}\left(\frac{1}{r}\right)+\frac{\partial}{\partial y}\left(\frac{\Phi_a-\Phi_b}{hV}\right)\right\}\frac{\partial}{\partial y}\left(\frac{1}{r}\right)dx\,dy \quad \ldots \quad (38)$$

$$=\frac{h}{4\pi}\cdot\frac{h}{14}\int_{x_1'-1}^{x_1'+1}\left\{\left(\frac{\Phi_a-\Phi_b}{hV}\right)_{y'=y_1'-1}+\left(\frac{\Phi_a-\Phi_b}{hV}\right)_{y'=y_1'+1}\right\}\frac{h}{28}\,\frac{dx'}{r^3}$$

$$+\frac{h}{4\pi}\cdot\frac{h}{28}\int_{y_1'-1}^{y_1'+1}\left\{\left(\frac{\Phi_a-\Phi_b}{hV}\right)_{x'=x_1'-1}+\left(\frac{\Phi_a-\Phi_b}{hV}\right)_{x'=x_1'+1}\right\}\frac{h}{14}\cdot\frac{dy'}{r^3}$$

$$-\frac{h}{4\pi}\int_{y_1'-1}^{y_1'+1}\int_{x_1'-1}^{x_1'+1}\left\{(x'-x_1')\frac{\partial}{\partial x'}\left(\frac{\Phi_a-\Phi_b}{hV}\right)+(y'-y_1')\frac{\partial}{\partial y'}\left(\frac{\Phi_a-\Phi_b}{hV}\right)\right\}\frac{h^2\,dx'\,dy'}{392r^3},$$

where $$\frac{r^3}{h^3}=\frac{1}{21952}\left\{(x'-x_1')^2+4(y'-y_1')^2\right\}^{3/2}.$$

Therefore, $$\frac{w_1}{V}=\frac{14}{\pi}(J_1+J_2-J_3), \quad \ldots \quad (39)$$

where

$$J_1=\int_{-1}^{1}\{G(\xi,-1)+G(\xi,1)\}\frac{d\xi}{(\xi^2+4)^{3/2}},$$

$$J_2=\int_{-1}^{1}\{G(-1,\eta)+G(1,\eta)\}\frac{d\eta}{(1+4\eta^2)^{3/2}},$$

$$J_3=\int_{-1}^{1}\int_{-1}^{1}\left(\xi\frac{\partial G}{\partial\xi}+\eta\frac{\partial G}{\partial\eta}\right)\frac{d\xi\,d\eta}{(\xi^2+4\eta^2)^{3/2}}.$$

From equation (29) with $\xi_1=0,\ \xi_2=\frac{1}{2},\ \xi_3=1$,

$$\int_0^1\frac{G(\xi)\,d\xi}{(\xi^2+4)^{3/2}}=2\,[G(0)\{I_2-\tfrac{3}{2}I_1+\tfrac{1}{2}I_0\}+G(\tfrac{1}{2})\{-2I_2+2I_1\}+G(1)\{I_2-\tfrac{1}{2}I_1\}],$$

where $I_2=0\cdot0339982$, $I_1=0\cdot0527864$, $I_0=0\cdot1118034$ are determined by substituting $\xi_1=0$, $\xi_3=1$, $\eta=1$ in equation (28).

Similarly

$$\int_0^1\frac{G(\eta)\,d\eta}{(1+4\eta^2)^{3/2}}=\frac{1}{8}\int_0^1\frac{G(\eta)\,d\eta}{(\eta^2+\frac{1}{4})^{3/2}}=\tfrac{1}{4}[G(0)\{I_2-\tfrac{3}{2}I_1+\tfrac{1}{2}I_0\}+G(\tfrac{1}{2})\{-2I_2+2I_1\}+G(1)\{I_2-\tfrac{1}{2}I_1\}],$$

where $I_2=0\cdot5492083$, $I_1=1\cdot1055728$, $I_0=3\cdot5777088$ are determined by substituting $\xi_1=0$, $\xi_3=1$, $\eta=\frac{1}{4}$ in equation (28). The integrals $\int_{-1}^{0}$ are treated in the same way, and it follows that

$$\left.\begin{aligned}J_1&=0\cdot0428812\{G(0,-1)+G(0,1)\}\\&\quad+0\cdot0751528\{G(-\tfrac{1}{2},-1)+G(-\tfrac{1}{2},1)+G(\tfrac{1}{2},-1)+G(\tfrac{1}{2},1)\}\\&\quad+0\cdot0152100\{G(-1,-1)+G(-1,1)+G(1,-1)+G(1,1)\}\\J_2&=0\cdot3398517\{G(-1,0)+G(1,0)\}\\&\quad+0\cdot2781823\{G(-1,-\tfrac{1}{2})+G(-1,\tfrac{1}{2})+G(1,-\tfrac{1}{2})+G(1,\tfrac{1}{2})\}\\&\quad-0\cdot0008945\{G(-1,-1)+G(-1,1)+G(1,-1)+G(1,1)\}\end{aligned}\right\} \quad \ldots \quad (40)$$

The general formula from which J_3 is evaluated is obtained by expressing $G(\xi, \eta)$ as a polynomial in powers of ξ and η in terms of the 16 values of G occurring in equation (40) on the perimeter of R and 9 other values inside R, as shown in Fig. 1. The method of derivation is explained in the Appendix to this report and leads to the formula

$$\begin{aligned} J_3 = &- 10\cdot7845628\,\{G(0, 0)\} + 2\cdot8338092\,\{G(-\tfrac{1}{2}, 0) + G(\tfrac{1}{2}, 0)\} \\ &+ 0\cdot4636337\,\{G(-1, 0)\} + G(1, 0)\} + 0\cdot7293835\,\{G(0, -\tfrac{1}{2}) + G(0, \tfrac{1}{2})\} \\ &+ 0\cdot3084028\,\{G(-\tfrac{1}{2}, -\tfrac{1}{2}) + G(-\tfrac{1}{2}, \tfrac{1}{2}) + G(\tfrac{1}{2}, -\tfrac{1}{2}) + G(\tfrac{1}{2}, \tfrac{1}{2})\} \\ &+ 0\cdot2422526\,\{G(-1, -\tfrac{1}{2}) + G(-1, \tfrac{1}{2}) + G(1, -\tfrac{1}{2}) + G(1, \tfrac{1}{2})\} \\ &+ 0\cdot0181922\,\{G(0, -1) + G(0, 1)\} \\ &+ 0\cdot0879315\,\{G(-\tfrac{1}{2}, -1) + G(-\tfrac{1}{2}, 1) + G(\tfrac{1}{2}, -1) + G(\tfrac{1}{2}, 1)\} \\ &+ 0\cdot0350445\,\{G(-1, -1) + G(-1, 1) + G(1, -1) + G(1, 1)\}\,. \end{aligned} \qquad (41)$$

From equations (39), (40) and (41), the contribution to w/V from the rectangle R is

$$\begin{aligned} w_1/V = &\ 48\cdot059661\,\{G(0, 0)\} - 12\cdot628413\,\{G(-\tfrac{1}{2}, 0) + G(\tfrac{1}{2}, 0)\} \\ &- 0\cdot551614\,\{G(-1, 0) + G(1, 0)\} - 3\cdot250380\,\{G(0, -\tfrac{1}{2}) + G(0, \tfrac{1}{2})\} \\ &- 1\cdot374347\,\{G(-\tfrac{1}{2}, -\tfrac{1}{2}) + G(-\tfrac{1}{2}, \tfrac{1}{2}) + G(\tfrac{1}{2}, -\tfrac{1}{2}) + G(\tfrac{1}{2}, \tfrac{1}{2})\} \\ &+ 0\cdot160115\,\{G(-1, -\tfrac{1}{2}) + G(-1, \tfrac{1}{2}) + G(1, -\tfrac{1}{2}) + G(1, \tfrac{1}{2})\} \\ &+ 0\cdot110023\,\{G(0, -1) + G(0, 1)\} \\ &- 0\cdot056946\,\{G(-\tfrac{1}{2}, -1) + G(-\tfrac{1}{2}, 1) + G(\tfrac{1}{2}, -1) + G(\tfrac{1}{2}, 1)\} \\ &- 0\cdot092375\,\{G(-1, -1) + G(-1, 1) + G(1, -1) + G(1, 1)\}\,. \end{aligned} \qquad (42)$$

Therefore the value of

$$\frac{w}{V} = \frac{w_0}{V} + \frac{w_1}{V} \qquad (43)$$

is obtained by summing the contributions (31) and (42).

4. *Potential Solutions at a Uniform Incidence.*—The values of the downwash angle w/V have been determined for the doublet distributions in equations (10a), (10b), (10c) and are expressed as linear functions of $A_1, A_2, \ldots A_{10}$ at each of the 10 positions, shown in Fig. 1, *viz.*,

$$(x_1', y_1') = (7, 0), (14, 0), (21, 0), (27, 0), (14, 3), (21, 3), (27, 3), (21, 7), (27, 7), (27, 10).$$

It remains to equate the 10 linear functions with the values of w/V required at the respective positions (x_1', y_1'). The investigation has been restricted to the uncambered wing in an inclined uniform stream, for which the simple boundary condition is expressed in equation (5),

$$w/V = \alpha\,. \qquad (44)$$

The simultaneous equations and solutions for $A_1, A_2, \ldots A_{10}$, when $\alpha = 1$, are set out in Tables 6A, 6B, 6C. The respective expressions for the velocity potential difference from equation (16) are

(*a*) $$\frac{\Phi_a - \Phi_b}{hV\alpha} = \Phi_0[B_1 + B_2(X - \tfrac{1}{2}X^2) + B_3(X - X^2 + \tfrac{1}{3}X^3) + B_4(X - \tfrac{3}{2}X^2 + X^3 - \tfrac{1}{4}X^4)]\,,$$

where
$$\begin{aligned} B_1 &= 0\cdot4872 + 4\cdot4548Y^2 - 11\cdot2068Y^4 + 10\cdot8383Y^6\,, \\ B_2 &= -1\cdot2550 + 6\cdot4203Y^2 - 4\cdot5878Y^4\,, \\ B_3 &= -3\cdot9237 + 8\cdot5248Y^2, \\ B_4 &= 0\cdot3372\,. \end{aligned} \qquad (45a)$$

(*b*) $$\frac{\Phi_a - \Phi_b}{hV\alpha} = \Phi_0 \left[B_1 \left\{ 1 - \frac{4}{3\pi}\left(1 - X\right)^{3/2} \right\} + B_2(X - \tfrac{1}{2}X^2) + B_3(X - X^2 + \tfrac{1}{3}X^3) + B_4(X - \tfrac{3}{2}X^2 + X^3 - \tfrac{1}{4}X^4) \right],$$

where
$$B_1 = 0\cdot9809 + 2\cdot2604Y^2 - 6\cdot7968Y^4 + 7\cdot3591Y^6,$$
$$B_2 = -1\cdot6520 + 10\cdot9844Y^2 - 10\cdot2620Y^4,$$
$$B_3 = -21\cdot2653 + 43\cdot1813Y^2,$$
$$B_4 = 0\cdot3227. \qquad \text{(45b)}$$

(*c*) $$\frac{\Phi_a - \Phi_b}{hV\alpha} = \Phi_0 \left[B_1 - B_2 \cdot \frac{4}{3\pi}(1 - X)^{3/2} + B_3(X - \tfrac{1}{2}X^2) + B_4(X - X^2 + \tfrac{1}{3}X^3) \right],$$

where
$$B_1 = 2\cdot0003 + 3\cdot0860Y^2 - 2\cdot5843Y^4 + 2\cdot9692Y^6,$$
$$B_2 = -3\cdot0590 - 0\cdot5432Y^2 + 6\cdot9848Y^4,$$
$$B_3 = 0\cdot3540 + 3\cdot0693Y^2,$$
$$B_4 = 0\cdot3295. \qquad \text{(45c)}$$

The three sets of values of B_1, B_2, B_3, B_4 are tabulated as functions of $y' = 12Y$ in Table 7.

The three distributions of non-dimensional circulation $K/hV\alpha$, obtained by substituting $X = x/h = 1$ in equations (45), are evaluated in Table 8, and the three solutions show agreement within about $\pm$ 1 per cent.

The positions of the chordwise centres of pressure are defined in equation (13) and given for solution (*a*) in equation (17). These local aerodynamic centres are hardly distinguishable when plotted in Fig. 2.

On the other hand the distributions of hinge moment, calculated for the elevon of flap chord ratio 0·15 from the formula (14), are plotted in Fig. 3 and show appreciable variation in the three cases. With reference to the remarks that follow equations (10) these differences are not surprising, as the condition at the trailing edge will inevitably be a most important factor in determining the hinge moment. The flexible solution (*c*) should naturally be regarded as the most reliable one.

The distributions of pressure difference have been calculated from equations (1) and (45) along four selected wing sections $y' = 0, 3, 7, 10$. Curves of $\dfrac{p_b - p_a}{\frac{1}{2}\rho V^2\alpha}$ against x' are shown in Fig. 4. Over most of the plan form the agreement between the three solutions is excellent. The only discrepancies worthy of comment appear near the apex of the delta wing (0, 0) and near the outboard trailing edge $(x', y') = (28, y')$ where $y' \geqslant 7$. The former discrepancy can only be attributed to the fact that the apex is rather isolated from the solving points, as shown in Fig. 1. The latter discrepancy suggests that the somewhat rigid enforcement of the condition (7) by solution (*b*) becomes increasingly unsatisfactory towards the tips. It is interesting to note how the total lifts at a given section become consistent in spite of small local variations in $(p_b - p_a)$. Throughout solution (*c*) is the most convincing one ; and the intrinsic accuracy of this particular solution is considered to be better than that indicated by the comparison of pressure distributions in Fig. 4.

5. *Comparison with Vortex-Lattice Theory.*—The method of this report has yielded three solutions, (*a*), (*b*), (*c*) for the aerodynamic loading on the delta wing in Fig. 1. These have been compared with solutions of the identical problem by vortex-lattice theory (R. & M. 2596[2], June, 1948), *viz.*, Solutions 33, 34, given respectively in Ref. 2, Tables 37, 38, of which the latter involves

an auxiliary function P to allow for discontinuities at the median section. The values for the lift slope and the position of the aerodynamic centre measured from the trailing edge are as follows :—

Solution	(a)	(b)	(c)	33	34	Experiment
$\partial C_L/\partial\alpha$	3·018	3·007	3·038	3·142	3·123	3·07
a.c.	$0\cdot469h$	$0\cdot466_5h$	$0\cdot467_5h$	$0\cdot477h$	$0\cdot469h$	$0\cdot467h$

The table shows a mean difference of $3\frac{1}{2}$ per cent between $\partial C_L/\partial\alpha$ as determined by the present method in equation (18) and by the use of the vortex lattice. It is stated in R. & M. 2596[2], section 6.5, that a factor

$$1 + 0\cdot029 \text{ (tangent of sweepback of quarter-chord)}$$

should be applied as a correction to the values of $\partial C_L/\partial\alpha$ obtained by a 126 vortex-lattice, *e.g.*, solutions 33, 34. This factor increases the discrepancy between the two methods from 3 per cent to 5 per cent.

The spanwise distributions of circulation according to lifting-line theory and lifting-surface solutions (*c*) and 34 are compared in Fig. 5. On the basis that solution (*c*) is correct, the use of a 126 vortex-lattice would apparently allow for about 85 per cent of the difference between the lifting-line and lifting-surface theories over most of the span, but for only 70 per cent of this difference at 0·8 span and less towards the tip. This is consistent with the conclusions of Jones (R. & M. 2225[3], 1946), who has shown that, for a rectangular wing ($A = 6$), Falkner's approximate downwash distributions agree well with the results of the exact lifting-surface theory for points along the mid-chord axis of the wing over the inner part of the span, but that Falkner's values are about 5 per cent low at 0·8 span and are likely to be in greater error towards the tip. Thus the circulation from vortex-lattice theory would be expected to be proportionately higher towards the tip. The discrepancy of nearly 3 per cent over the inner part of the span is presumably due to an error associated with sweepback. However, for a given C_L, the spanwise distributions of lift in Table 9 according to solutions (*c*) and 34 differ by less than $\frac{1}{2}$ per cent inboard of 0·8 span.

Fig. 2 gives the loci of the chordwise centres of pressure along sections of the delta wing for each solution. Apart from the neighbourhood of the median section and the extreme tips the two methods are in excellent agreement. However vortex-lattice theory introduces fictitious kinks at the median section, which arise as a direct consequence of the use of the parameter θ given by

$$\cos\theta = \frac{14 + |y'| - x'}{14 - |y'|}$$

in the general form for the pressure distribution (R. & M. 2596[2], section 4)

$$\frac{p_b - p_a}{\frac{1}{2}\rho V^2} = \frac{2k}{V} = \frac{16s}{c}\,(F_0 \cot \tfrac{1}{2}\theta + F_1 \sin\theta)\,, \qquad \ldots \quad \ldots \quad \ldots \quad \ldots \quad (46)$$

where F_0, F_1 are functions of y only. The results suggest that, when F_0, F_1 contain the auxiliary function (Ref. 2, sections 4, 6.4) $P = 0\cdot65P_a + 0\cdot35P_b$, as is the case in solution 34, the centres of pressure near the median section are greatly improved. The above table shows that theoretical positions of the aerodynamic centre are determined in close agreement by the present method and solution 34. But it is clear that the use of P will not fully overcome the difficulty at the median section (R. & M. 2721[1], section 4.2).

A more detailed comparison of these solutions is given by the distributions of pressure difference at the four sections $y' = 0, 3, 7, 10$. Solutions (*a*), (*b*), and (*c*) are shown in Fig. 4 and solutions (*c*), 33 and 34 in Fig. 6. The only region in which the disparities in Fig. 6 adversely contrast those in Fig. 4 is along the median section $y' = 0$. Elsewhere the agreement is fairly good. It is shown in R. & M. 2721[1], section 4.2, that a solution of the form (46) can never satisfy the boundary conditions along $y' = 0$, as it necessarily produces infinite downwash there. It is therefore to be expected that the local pressures so determined will be in serious error and this is borne out by the results in Fig. 6. Solutions 33 and 34 also tend to give excessive pressure differences near the leading and trailing edges and to underestimate the values at the central part of the chord. It is noteworthy that it would appear from Fig. 6 as if the lift from these solutions were less than that from the present method. In fact the excessive lift near the leading edge is enough to provide the higher lift per unit span or circulation, as shown in Fig. 5. The disparities might well be reduced by considering further Fourier terms $F_2 \sin 2\theta$ and $F_3 \sin 3\theta$ in equation (46). By thus increasing the number of terms in the chordwise loading of the vortex-lattice theory from two to four a fairer comparison with the present method would be achieved. But a remedy for the singularity at the median section must apparently be based on the considerations in R. & M. 2721[1].

6. *Comparison with Experiment.*—A complete model of the delta wing of RAE 102 section 10 per cent thick[4] was tested at low speed in the National Physical Laboratory Duplex Wind Tunnel. Measurements included the total lift and pitching moment at a Reynolds number of 10^6 and pressure plotting at six sections of the wing. When corrected for tunnel interference, the tests covered an approximate range of incidence $-4\frac{1}{2}$ deg $< \alpha < +4$ deg.

The estimated free-stream lift slope and aerodynamic centre were

$$\partial C_L/\partial \alpha = 3\cdot 07$$

$$\text{a.c.} = 0\cdot 467h \text{ (from trailing edge).}$$

Both values compare well with the present solution(*c*), as the table in section 5 shows.

The corresponding distributions of pressure difference per radian incidence $(p_b - p_a)/\frac{1}{2}\rho V^2\alpha$ were obtained at sections

$$y' = 12\eta = 0,\ 0\cdot 44,\ 2\cdot 77,\ 5\cdot 54,\ 8\cdot 02,\ 11\cdot 08.$$

The experimental points for the section $y' = 0$ are plotted in Fig. 6. The estimated distributions at sections $y' = 3, 7, 10$, interpolated from the experimental data are also compared with the theoretical curves in Fig. 6.

Although these pressure distributions are influenced by wing section, it is important to note that the disparities between the theoretical curves of solution (*c*) and the experimental ones are similar at all sections. The limitations of the vortex-sheet theory are shown by the divergence at the leading edge, a marked discontinuity in the experimental pressure gradients at mid-chord associated with RAE 102 section, and, as would be expected, a discrepancy close to the trailing edge due to viscous flow. The curves so far given by vortex-lattice theory appear to be incorrect in shape at the median section, although the two theories are in fair agreement elsewhere.

These comparisons distinctly encourage the extension of the present calculations to allow for wing thickness and boundary layers and the application of similar methods to other plan forms.

7. *Concluding Remarks.*—Three approximate potential solutions for the pressure difference across a delta wing (Fig. 1) in an inclined uniform stream have been obtained. The solutions differ essentially in the manner in which the pressure difference is allowed to approach zero at the trailing edge. The lift slope and the position of the aerodynamic centre relative to the trailing edge are determined within 1 per cent and $\frac{1}{2}$ per cent respectively. The spanwise distributions of lift (Table 8) and centre of pressure (Fig. 2) are in excellent agreement. The pressure differences compare well over most of the plan form (Fig. 4) but there are understandable

discrepancies, which become appreciable near the apex of the delta wing and the outboard trailing edge. The distributions of hinge moment, calculated for the elevon of flap chord ratio 0·15, vary a good deal (Fig. 3). This is not surprising, as the essential distinctions between the solutions concern the trailing edge (equation (10) *et seq.*), but serves to emphasize the inherent difficulties in estimating hinge moments theoretically. It is quite clear that solution (*c*) is more flexible than the other two and in every respect more convincing; it is claimed that the intrinsic accuracy of this particular solution is at least as good as that indicated by its comparison with solutions (*a*) and (*b*) in Fig. 4.

On the basis of this claim certain conclusions with regard to the accuracy of the vortex-lattice theory (R. & M. 2596[2]) have been reached.

(*a*) The calculated values of $\partial C_L/\partial \alpha$ are about 3 per cent too great (or 5 per cent if the suggested correction factor in R. & M. 2596[2], section 6.5 is used). This disparity is probably associated with an error due to sweepback (Fig. 5).

(*b*) For a given C_L, the spanwise distribution of lift from vortex-lattice theory compares very well over most of the span but becomes too great towards the tips, as the conclusions of R. & M. 2225[3] would suggest (Table 9).

(*c*) The use of the auxiliary function P is necessary in the determination of the aerodynamic centre and leads to a very satisfactory estimate of its theoretical position.

(*d*) Fig. 6 shows notable discrepancies in the distribution of pressure difference, as calculated in R. & M. 2596[2] at the median section. This suggests that the mathematical form of the doublet distribution near the median section of a delta wing is of some importance (R. & M. 2721).

It is intended that the calculations of downwash in this report will serve in an extension of the theory to allow for wing thickness to the first order and further to provide an estimate of the pressure distribution on the delta wing in viscous incompressible flow. In the opinion of the author the only practicable approach to this problem is to assume a cambered lifting surface with the required two-dimensional characteristics at each section and to adjust the boundary condition expressed in equation (44). It would then be possible to make a direct comparison between a calculated distribution of pressure difference and the results from pressure-plotting experiments on the delta wing in the N.P.L. Duplex Wind Tunnel. Comparisons of lift, aerodynamic centre and pressure distributions suggest a favourable measure of agreement between these tests and the calculations for the thin delta wing in inviscid flow.

It is generally agreed that the aerodynamic characteristics associated with a swept trailing edge present a more crucial problem than that of the delta wing. It is recommended that a theoretical approach on the lines suggested in Ref. 1 should form the basis of a similar comparison with pressure-plotting experiments on a Vee wing.

8. *Acknowledgement.*—The author is greatly indebted to Miss J. Elliott and Miss E. Tingle for their help in carrying out most of the laborious numerical work of this report.

REFERENCES

No.	*Author*	*Title, etc.*
1	H. C. Garner	Methods of Approaching an Accurate Three-dimensional Potential Solution for a Wing. R. & M. 2721. October, 1948.
2	V. M. Falkner	Calculated Loadings due to Incidence of a Number of Straight and Swept-back Wings. R. & M. 2596. June, 1948.
3	W. P. Jones	Note on Lifting Plane Theory with Special Reference to Falkner's Approximate Method and a Proposed Electrical Device for Measuring Downwash Distributions. R. & M. 2225. May, 1946.
4	R. C. Pankhurst and H. B. Squire	Calculated Pressure Distributions for the RAE 100–104 Aerofoil Sections. C.P. 80. March, 1950.

TABLE 1

Values of Φ_0 [from equation (8)]

x' \ y'	0	½	1	2	2½	3	3½	4	5	6
0	0									
1	0·18673246	0								
2	·26089788	0·22711921	0							
3	·31563658	·29853766	0·23827773							
4	·35996615	·34930044	·31447898	0						
5	·39742372	·39001073	·36655468	0·24453125	0					
6	·42984504	·42432925	·40716230	·32642538	0·24462442	0				
6½	·44452899	·43968061	·42467460	·35608722	·32782928	0·17727515				
7	·45833333	·45402774	·44076072	·38140735	·38364104	·24358300				
7½	·47133942	·46748134	·45563619	·40352043	·42578379	·29053941	0			
8	·48361557	·48013082	·46946382	·42315371	·45950858	·32737650	0·24162967	0		
9	·50620242	·50329879	·49445549	·45681831	·42578379	·38363172	·32546477	0·23888101		
10	·52646961	·52399371	·51647529	·48493043	·45950858	·42594325	·38178805	·32228478	0	
11	·54470441	·54254933	·53602234	·50892346	·48744035	·45960734	·42403229	·37834458	0·23118689	
12	·56113172	·55922288	·55345329	·52969054	·51108199	·48729769	·45748131	·42028685	·31250551	0
13	·57593268	·57421575	·56903442	·54782772	·53137665	·51056168	·48482878	·45335235	·36712612	0·22059525
13½	·58277069	·58113383	·57619743	·55604599	·54047455	·52085372	·49673186	·46744944	·38879414	·26410363
14	·58925565	·58769009	·58297152	·56375418	·54895598	·53037715	·50764696	·48023328	·40777482	·29833478
14½	·59540229	·59390036	·58937595	·57098767	·55687154	·53920590	·51768467	·49187505	·42456806	·32652320
15	·60122416	·59977907	·59542803	·57777730	·56426457	·54740215	·52693618	·50251227	·43953994	·35036926
16	·61194248	·61059391	·60653678	·59013016	·57762811	·56210119	·54337300	·52120242	·46506550	·38880932
17	·62149975	·62022882	·61640771	·60099457	·58928317	·57481490	·55743677	·53699231	·48592327	·41852676
18	·62997293	·62876453	·62513332	·61051567	·59945063	·58580097	·56947976	·55037155	·50312966	·44207325
19	·63742906	·63627098	·63279244	·61881172	·60825344	·59525946	·57976871	·56170098	·51738149	·46097840
20	·64392705	·64280932	·63945306	·62598072	·61582491	·60334917	·58851084	·57125434	·52917783	·47623024
20½	·64683328	·64573253	·64242772	·62916882	·61918144	·60692186	·59235454	·57543337	·53427458	·48272664
21	·64951905	·64843342	·64517438	·63210504	·62226696	·61019861	·59587051	·57924443	·53888855	·48854428
21½	·65199002	·65091779	·64769932	·63479779	·62509164	·61319199	·59907443	·58270739	·54305252	·49374895
22	·65425150	·65319111	·65000844	·63725490	·62766488	·61591349	·60198055	·58584011	·54679543	·49838977
23	·65816602	·65712510	·65400134	·64149080	·63209105	·62058200	·60695008	·59117786	·55311822	·50614544
24	·66130008	·66027376	·65719415	·64486537	·63560745	·62427875	·61086998	·59536963	·55803161	·51209424
25	·66368762	·66267176	·65962375	·64742484	·63826185	·62706753	·61381695	·59850866	·56167692	·51645757
26	·66535950	·66435056	·66132341	·64921009	·64011993	·62900343	·61585642	·60067347	·56417017	·51941194
26½	·66593598	·66492931	·66190905	·64982394	·64075567	·62966680	·61655376	·60141182	·56501555	·52040653
27	·66634391	·66533882	·66232330	·65025760	·64120438	·63013450	·61704476	·60193093	·56560783	·52110040
27½	·66658647	·66558227	·66256950	·65051504	·64147053	·63041173	·61733533	·60223770	·56595669	·52150748
28	0·66666667	0·66566278	0·66265089	0·65060006	0·64155835	0·63050298	0·61743103	0·60233861	0·56607111	0·52164054

TABLE 1—*continued*

Values of Φ_0 [from equation (8)]

x' \ y'	6½	7	7½	8	9	9½	10	10½	11	11½	12
0											
1											
2											
3											
4											
5											
6											
6½											
7											
7½											
8											
9											
10											
11											
12											
13	0										
13½	0·15503525										
14	·21415293	0									
14½	·25637053	0·14979484									
15	·28955074	·20688003	0								
16	·33986234	·27955353	0·19870221	0							
17	·37684555	·32784453	·26824679	0·18951924							
18	·40524200	·36312421	·31420383	·25549799	0						
19	·42754325	·38998892	·34751981	·29878556	0·16754293	0					
20	·44524810	·41086107	·37262954	·32985991	·22457734	0·15429307	0				
20½	·45269661	·41952958	·38288256	·34224347	·24505052	·18377134	0·10133233				
21	·45933681	·42720256	·39187695	·35297622	·26169512	·20641125	·13903830	0			
21½	·46524562	·43398707	·39976761	·36229605	·27561870	·22452225	·16524382	0·08851091			
22	·47048854	·43997252	·40668074	·37038969	·28735659	·23932652	·18518081	·12110573	0		
23	·47919412	·44983738	·41797452	·38346932	·30569578	·26175492	·21367250	·16032754	0·09921376	0	
24	·48582019	·45728015	·42640878	·39311852	·31875382	·27726805	·23246704	·18377647	·13023869	0·07012951	
25	·49064793	·46266244	·43245619	·39996849	·32777702	·28777625	·24483718	·19849875	·14789429	·09091706	0
26	·49389774	·46626213	·43647139	·40447892	·33359250	·29444970	·25254010	·20740880	·15808946	·10179764	0
26½	·49498731	·46746356	·43780475	·40596825	·33548570	·29660202	·25499512	·21020337	·16121246	·10500057	0
27	·49574558	·46829745	·43872750	·40699556	·33678116	·29806728	·25665616	·21207855	·16328452	·10708961	0
27½	·49618945	·46878437	·43926485	·40759198	·33753224	·29890790	·25760351	·21314093	·16444753	·10824640	0
28	0·49633425	0·46894286	0·43943934	0·40778516	0·33776812	0·29917746	0·25790598	0·21347815	0·16481396	0·10860717	0

TABLE 2A

Values of $\int_{Y}^{1} \Phi_0 P \, dX$ [from equation (15)]

$y' = 12Y$ \ P	1	$X - \frac{1}{2}X^2$	$X - X^2 + \frac{1}{3}X^3$	$X - \frac{3}{2}X^2 + X^3 - \frac{1}{4}X^4$	$\frac{4}{3\pi}(1 - X)^{3/2}$
0	0·533333	0·198942	0·146994	0·116284	0·072915
1	·506430	·195549	·144119	·113757	·063887
2	·463347	·186350	·136502	·107205	·052196
3	·412961	·172524	·125359	·097857	·040867
4	·358690	·155009	·111546	·086464	·030723
5	·302868	·134848	·096046	·073952	·022090
6	·247346	·113015	·079647	·060941	·015070
7	·193895	·090581	·063170	·048066	·009632
8	·143933	·068510	·047298	·035821	·005651
9	·098910	·047814	·032701	·024674	·002942
10	·060136	·029433	·019962	·015021	·001274
11	0·028684	0·013914	0·009029	0·006395	0·000393
12	0	0	0	0	0

TABLE 2B

Values of $\int_{Xh}^{1} \Phi_0 P \, dX$ [from equation (15)]

y' \ P	1	$X - \frac{1}{2}X^2$	$X - X^2 + \frac{1}{3}X^3$	$X - \frac{3}{2}X^2 + X^3 - \frac{1}{4}X^4$	$\frac{4}{3\pi}(1 - X)^{3/2}$
0	0·099707	0·049481	0·033208	0·024924	0·000982
2	·083454	·041497	·027803	·020862	·000652
4	·064370	·032078	·021461	·016100	·000383
6	·044621	·022256	·014871	·011155	·000190
8	·026159	·013062	·008719	·006540	·000072
9	·018055	·009019	·006018	·004514	·000038
10	·011028	·005510	·003676	·002757	·000017
11	0·005285	0·002641	0·001762	0·001321	0·000005
12	0	0	0	0	0

TABLE 3

Values of $\dfrac{1}{(\xi^2 + 4\eta^2)^{3/2}}$ [from equation (23)]

ξ \ η	0	$\frac{1}{2}$	1	2	3	4	5	6	7	8	9	10
0	∞	1·00000000	0·12500000	0·01562500	0·00462963	0·00195313	0·00100000	0·00057870	0·00036443	0·00024414	0·00017147	0·00012500
1	1·00000000	0·35355340	·08944272	·01426680	·00444322	·00190822	·00098519	·00057273	·00036166	·00024272	·00017068	·00012453
2	0·12500000	·08944272	·04419418	·01118034	·00395285	·00178335	·00094287	·00055540	·00035355	·00023853	·00016834	·00012315
3	·03703704	·03162278	·02133462	·00800000	·00331269	·00160330	·00087874	·00052840	·00034070	·00023181	·00016456	·00012089
4	·01562500	·01426680	·01118034	·00552427	·00266683	·00139754	·00080041	·00049411	·00032396	·00022292	·00015951	·00011786
5	·00800000	·00754293	·00640329	·00380911	·00209897	·00119101	·00071554	·00045517	·00030438	·00021230	·00015338	·00011413
6	·00462963	·00444322	·00395285	·00266683	·00163682	·00100000	·00063051	·00041409	·00028299	·00020041	·00014640	·00010984
7	·00291545	·00282843	·00259171	·00190823	·00127606	·00083250	·00054982	·00037296	·00026077	·00018774	·00013882	·00010511
8	·00195313	·00190823	·00178335	·00139754	·00100000	·00069053	·00047614	·00033335	·00023853	·00017469	·00013084	·00010005
9	·00137174	·00134673	·00127606	·00104675	·00079017	·00057273	·00041066	·00029630	·00021691	·00016164	·00012269	·00009479
10	·00100000	·00098519	·00094287	·00080041	·00063051	·00047614	·00035355	·00026237	·00019636	·00014888	·00011454	·00008944
11	·00075131	·00074210	·00071554	·00062362	·00050834	·00039741	·00030438	·00023181	·00017718	·00013661	·00010653	·00008409
12	·00057870	·00057273	·00055540	·00049411	·00041409	·00033335	·00026237	·00020460	·00015951	·00012500	·00009877	·00007881
13	·00045517	·00045116	·00043947	·00039741	·00034070	·00028117	·00022666	·00018059	·00014340	·00011413	·00009135	·00007368
14	·00036443	·00036166	·00035355	·00032396	·00028299	·00023853	·00019636	·00015951	·00012885	·00010406	·00008433	·00006873
15	·00029630	·00029433	·00028857	·00026729	·00023716	·00020354	·00017068	·00014108	·00011576	·00009479	·00007774	·00006400
16	·00024414	·00024272	·00023853	·00022292	·00020041	·00017469	·00014888	·00012500	·00010406	·00008632	·00007159	·00005952
17	·00020354	·00020249	·00019939	·00018774	·00017068	·00015078	·00013034	·00011099	·00009362	·00007860	·00006589	·00005529
18	·00017147	·00017068	·00016834	·00015951	·00014640	·00013084	·00011454	·00009877	·00008433	·00007159	·00006061	·00005133
19	·00014579	·00014519	·00014340	·00013661	·00012642	·00011413	·00010103	·00008812	·00007607	·00006525	·00005578	·00004763
20	·00012500	·00012453	·00012315	·00011786	·00010984	·00010005	·00008944	·00007881	·00006873	·00005952	·00005133	·00004419
21	·00010798	·00010761	·00010653	·00010236	·00009599	·00008812	·00007947	·00007068	·00006220	·00005434	·00004726	·00004100
22	·00009391	·00009362	·00009276	·00008944	·00008433	·00007795	0·00007086	·00006354	·00005639	·00004968	·00004354	·00003805
23	·00008219	·00008196	·00008127	·00007860	·00007446	·00006925		·00005728	·00005123	·00004547	·00004014	·00003532
24	·00007234	·00007215	·00007159	0·00006942	·00006605	0·00006176		0·00005176	·00004662	0·00004167	0·00003704	·00003280
25	·00006400	·00006385	0·00006339		·00005884				·00004251			·00003047
26	0·00005690	0·00005677			0·00005264				0·00003884			0·00002833

ξ \ η	11	12	13	14	15	16	17	18	19	20	21
0	0·00009391	0·00007235	0·00005690	0·00004555	0·00003704	0·00003052	0·00002544	0·00002143	0·00001822	0·00001562	0·00001350
1	·00009362	·00007215	·00005677	·00004547	·00003698	·00003047	·00002541	·00002141	·00001821	·00001561	·00001349
2	·00009276	·00007159	·00005639	·00004521	·00003679	·00003034	·00002531	·00002133	·00001815	·00001557	·00001345
3	·00009135	·00007069	·00005578	·00004478	·00003649	·00003012	·00002515	·00002121	·00001806	·00001549	·00001339
4	·00008944	·00006942	·00005493	·00004419	·00003607	·00002982	·00002492	·00002104	·00001793	·00001539	·00001332
5	·00008708	·00006787	·00005388	·00004346	·00003555	·00002943	·00002464	·00002083	·00001776	·00001527	·00001322
6	·00008433	·00006605	·00005264	·00004259	·00003492	·00002898	·00002430	·00002057	·00001756	·00001511	0·00001309
7	·00008127	·00006400	·00005123	·00004159	·00003421	·00002845	·00002391	·00002027	·00001733	·00001493	
8	·00007795	·00006176	·00004968	·00004049	·00003341	·00002786	·00002347	·00001994	·00001708	0·00001473	
9	·00007446	·00005940	·00004801	·00003931	·00003255	·00002722	·00002299	·00001957	·00001679		
10	·00007086	·00005690	·00004626	·00003805	·00003162	·00002654	·00002247	·00001917	0·00001648		
11	.00006720	·00005434	·00004444	·00003673	·00003065	·00002581	·00002191	·00001875			
12	.00006354	·00005176	·00004259	·00003537	·00002983	·00002505	·00002133	0·00001830			
13	.00005993	·00004918	·00004071	·00003399	·00002861	·00002427	·00002073				
14	·00005639	·00004662	·00003884	·00003260	·00002756	·00002347	0·00002012				
15	·00005297	·00004412	·00003698	·00003120	·00002650	·00002265					
16	·00004968	·00004167	·00003515	·00002982	·00002544	0·00002184					
17	·00004653	·00003931	·00003336	·00002845	·00002439						
18	·00004354	·00003704	·00003162	·00002711	0·00002335						
19	·00004071	·00003486	·00002995	·00002581							
20	·00003805	·00003280	·00002833	0·00002454							
21	·00003555	·00003084	·00002679								
22	·00003320	·00002898	0·00002531								
23	·00003102	.00002722									
24	0·00002898	0·00002558									
25											
26											

TABLE 4

Values of $\frac{1}{4(y' - y_1')^2}\left\{1 - \frac{28 - x_1'}{\sqrt{\{(28 - x_1')^2 + 4(y' - y_1')^2\}}}\right\}$ [from equation (27)]

$\lvert y' - y_1' \rvert$ \ x_1'	7	14	21	27
0	0·00113379	0·00255102	0·01020408	0·50000000
½	·00113186	·00254130	·01005050	·29289324
1	·00112613	·00251263	·00961901	·13819660
2	·00110384	·00240475	·00823480	·04734152
3	·00106878	·00224597	·00668732	·02321114
4	·00102363	·00205870	·00533587	·01368696
5	·00097140	·00186266	·00426538	·00900496
6	·00091498	·00167183	·00344534	·00636774
7	·00085689	·00149435	·00282034	·00473853
8	·00079910	·00133397	·00234055	·00366258
9	·00074304	·00119154	·00196776	·00291522
10	·00068966	·00106634	·00167412	·00237515
11	·00064132	·00095687	·00143966	·00197230
12	·00059287	·00086134	·00125000	·00166384
13	·00054980	·00077796	·00109471	·00142244
14	·00051020	·00070508	·00096615	·00122999
15	·00047393	·00064124	·00085863	·00107409
16	·00044076	·00058514	·00076787	·00094508
17	·00041047	·00053568	·00069061	·00083962
18	·00038282	·00049194	·00062433	·00075018
19	·00035756	·00045311	·00056706	·00067430
20	·00033448	·00041853	·00051726	·00060938
21	·00030742	·00038763	·00047370	·00055340
22	0·00028939	0·00035992	0·00043537	0·00050479

TABLE 5

Values of C_n [from equation (29)]

Integral	ξ	$\lvert\eta\rvert = 0$	$\lvert\eta\rvert = \frac{1}{2}$	$\lvert\eta\rvert = 1$	$\lvert\eta\rvert = 1\frac{1}{2}$	$\lvert\eta\rvert = 2$	$\lvert\eta\rvert = 3$
$\int_{-5}^{-3}$	−5	0·0020795	0·0020409	0·0018687			
	−4	0·0225076	0·0203377	0·0155976			
	−3	0·0109684	0·0095188	0·0066403			
$\int_{-3}^{-1}$	−3	−0·0062495	0·0030062	0·0057713	0·0041649	0·0026463	0·0011106
	−2	0·2347213	0·1432901	0·0621117	0·0287647	0·0149016	0·0052505
	−1	0·2159726	0·0952802	0·0283262	0·0105014	0·0047936	0·0014949
$\int_{-1}^{+1}$	−1			0·0152100	0·0053393	0·0023973	0·0007433
	−½			0·0751528	0·0235324	0·0101342	0·0030488
	0			0·0428812	0·0125294	0·0052540	0·0015490
	½			0·0751528	0·0235324	0·0101342	0·0030488
	1			0·0152100	0·0053393	0·0023973	0·0007433
$\int_{+1}^{+3}$	1	0·2159726	0·0952802	0·0283262	0·0105014	0·0047936	0·0014949
	2	0·2347213	0·1432901	0·0621117	0·0287647	0·0149016	0·0052505
	3	−0·0062495	0·0030062	0·0057713	0·0041649	0·0026463	0·0011106
$\int_{+3}^{+5}$	3	0·0109684	0·0095188	0·0066403			
	4	0·0225076	0·0203377	0·0155976			
	5	0·0020795	0·0020409	0·0018687			

TABLE 6A

Simultaneous Equations and Solution (a)

(x_1', y_1')	A_1	A_2	A_3	A_4	A_5	A_6	A_7	A_8	A_9	A_{10}	w/V
(7, 0)	0·982422	0·113302	0·133984	0·138595	−0·062115	−0·020952	−0·016014	−0·009059	−0·004116	−0·003844	1
(14, 0)	·726192	·258320	·222552	·183883	− ·105478	− ·043649	− ·032051	− ·016099	− ·007460	− ·006439	1
(21, 0)	·638820	·329748	·227718	·167470	− ·136008	− ·063817	− ·044309	− ·023531	− ·011331	− ·009640	1
(27, 0)	·576631	·323578	·199627	·146518	− ·151608	− ·074386	− ·050205	− ·028566	− ·014045	− ·025488	1
(14, 3)	·770684	·256678	·222345	·185047	+ ·008890	− ·002434	+ ·000914	− ·024275	− ·010983	− ·009960	1
(21, 3)	·629305	·320416	·222290	·164067	− ·041636	− ·018880	− ·012868	− ·041589	− ·019786	− ·016577	1
(27, 3)	·557285	·311290	·192549	·141462	− ·063756	− ·029362	− ·020777	− ·050519	− ·024821	− ·020837	1
(21, 7)	·577980	·276912	·196639	·148992	+ ·332465	+ ·155363	+ ·110169	+ ·083789	+ ·038496	− ·001456	1
(27, 7)	·459141	·251676	·157384	·116008	+ ·268046	+ ·139114	+ ·090065	+ ·039643	+ ·021589	− ·031036	1
(27, 10)	0·280827	0·151987	0·096017	0·070989	+0·495631	+0·252034	+0·165786	+0·410565	+0·207667	+0·290213	1

Solution $A_1 = 0\cdot4872$ $A_2 = 4\cdot4548$ $A_3 = -11\cdot2068$ $A_4 = 10\cdot8383$ $A_5 = -1\cdot2550$ $A_6 = 6\cdot4203$ $A_7 = -4\cdot5878$ $A_8 = -3\cdot9237$
$A_9 = 8\cdot5248$ $A_{10} = 0\cdot3372$

TABLE 6B

Simultaneous Equations and Solution (b)

(x_1', y_1')	A_1	A_2	A_3	A_4	A_5	A_6	A_7	A_8	A_9	A_{10}	w/V
(7, 0)	0·624305	0·113302	0·133984	0·138595	−0·051494	−0·020952	−0·016014	−0·008557	−0·004116	−0·003749	1
(14, 0)	·579668	·258320	·222552	·183883	− ·094381	− ·043649	− ·032051	− ·015318	− ·007460	− ·006276	1
(21, 0)	·619630	·329748	·227718	·167470	− ·129741	− ·063817	− ·044309	− ·022878	− ·011331	− ·009473	1
(27, 0)	·629904	·323578	·199627	·146518	− ·149313	− ·074386	− ·050205	− ·028178	− ·014045	− ·025368	1
(14, 3)	·611438	·256678	·222345	·185047	+ ·000782	− ·002434	+ ·000914	− ·022772	− ·010983	− ·009454	1
(21, 3)	·606627	·320416	·222290	·164067	− ·040312	− ·018880	− ·012868	− ·040090	− ·019786	− ·016125	1
(27, 3)	·606757	·311290	·192549	·141462	− ·059697	− ·029362	− ·020777	− ·049755	− ·024821	− ·020615	1
(21, 7)	·541349	·276912	·196639	·148992	+ ·310878	+ ·155363	+ ·110169	+ ·077155	+ ·038496	− ·002670	1
(27, 7)	·492976	·251676	·157384	·116008	+ ·276249	+ ·139114	+ ·090065	+ ·042632	+ ·021589	− ·029737	1
(27, 10)	0·298135	0·151987	0·096017	0·070989	+0·502029	+0·252034	+0·165786	+0·414068	+0·207607	+0·292418	1

Solution $A_1 = 0{\cdot}9809$ $A_2 = 2{\cdot}2604$ $A_3 = -6{\cdot}7968$ $A_4 = 7{\cdot}3591$ $A_5 = -1{\cdot}6520$ $A_6 = 10{\cdot}9844$ $A_7 = -10{\cdot}2620$ $A_8 = -21{\cdot}2653$
$A_9 = 43{\cdot}1813$ $A_{10} = 0{\cdot}3227$

TABLE 6C

Simultaneous Equations and Solution (c)

(x_1', y_1')	A_1	A_2	A_3	A_4	A_5	A_6	A_7	A_8	A_9	A_{10}	w/V
(7, 0)	0·982422	−0·358117	0·113302	0·133984	−0·062115	+0·010621	−0·020952	−0·009059	+0·0005018	−0·003844	1
(14, 0)	·726192	− ·146524	·258320	·222552	− ·105478	+ ·011097	− ·043649	− ·016099	+ ·0007807	− ·006439	1
(21, 0)	·638820	− ·019190	·329748	·227718	− ·136008	+ ·006267	− ·063817	− ·023531	+ ·0006529	− ·009640	1
(27, 0)	·576631	+ ·053273	·323578	·199627	− ·151608	+ ·002295	− ·074386	− ·028566	+ ·0003881	− ·025488	1
(14, 3)	·770684	− ·159246	·256678	·222345	+ ·008890	− ·008108	− ·002434	− ·024275	+ ·0015033	− ·009960	1
(21, 3)	·629305	− ·022678	·320416	·222290	− ·041636	+ ·001324	− ·018880	− ·041589	+ ·0014988	− ·016577	1
(27, 3)	·557285	+ ·049472	·311290	·192549	− ·063756	+ ·004059	− ·029362	− ·050519	+ ·0007637	− ·020837	1
(21, 7)	·577980	− ·036631	·276912	·196639	+ ·332465	− ·021587	+ ·155363	+ ·083789	− ·0066336	− ·001456	1
(27, 7)	·459141	+ ·033835	·251676	·157384	+ ·268046	+ ·008203	+ ·139114	+ ·039643	+ ·0029889	− ·031036	1
(27, 10)	0·280827	+0·017308	0·151987	0·096017	+0·495631	+0·006398	+0·252034	+0·410565	+0·0035025	+0·290213	1

Solution $A_1 = 2{\cdot}0003$ $A_2 = 3{\cdot}0860$ $A_3 = -2{\cdot}5843$ $A_4 = 2{\cdot}9692$ $A_5 = -3{\cdot}0590$ $A_6 = -0{\cdot}5432$ $A_7 = 6{\cdot}9848$ $A_8 = 0{\cdot}3540$
$A_9 = 3{\cdot}0693$ $A_{10} = 0{\cdot}3295$

TABLE 7

Values of B_1, B_2, B_3, B_4 for Solutions (a), (b), (c)

Solution (a) from equation (45a)

y'	B_1	B_2	B_3	B_4
0	+0·4872	4·4548	−11·2068	10·8383
1	0·4782	4·4998	−11·2387	10·8383
2	0·4493	4·6397	−11·3342	10·8383
3	0·3935	4·8894	−11·4935	10·8383
4	0·2997	5·2734	−11·7166	10·8383
5	+0·1528	5·8264	−12·0033	10·8383
6	−0·0666	6·5927	−12·3538	10·8383
7	−0·3809	7·6266	−12·7679	10·8383
8	−0·8161	8·9922	−13·2458	10·8383
9	−1·4003	10·7635	−13·7874	10·8383
10	−2·1637	13·0245	−14·3928	10·8383
11	−3·1377	15·8687	−15·0618	10·8383
12	−4·3544	19·3999	−15·7946	10·8383

Solution (b) from equation (45b)

y'	B_1	B_2	B_3	B_4
0	+ 0·9809	2·2604	− 6·7968	7·3591
1	0·9684	2·3387	− 6·8680	7·3591
2	0·9186	2·5988	− 7·0818	7·3591
3	0·7946	3·1156	− 7·4381	7·3951
4	0·5352	4·0140	− 7·9370	7·3591
5	+ 0·0548	5·4689	− 8·5784	7·3591
6	− 0·7562	7·7053	− 9·3623	7·3591
7	− 2·0309	10·9980	−10·2887	7·3591
8	− 3·9256	15·6720	−11·3577	7·3591
9	− 6·6194	22·1019	−12·5692	7·3591
10	−10·3135	30·7128	−13·9232	7·3591
11	−15·2305	41·9792	−15·4197	7·3591
12	−21·6137	56·4261	−17·0588	7·3591

Solution (c) from equation (45c)

y'	B_1	B_2	B_3	B_4
0	+ 2·0003	3·0860	−2·5843	2·9692
1	1·9791	3·0824	−2·5358	2·9692
2	1·9156	3·0733	−2·3903	2·9692
3	1·8106	3·0640	−2·1478	2·9692
4	1·6653	3·0635	−1·8082	2·9692
5	1·4816	3·0842	−1·3717	2·9692
6	1·2629	3·1420	−0·8381	2·9692
7	1·0134	3·2565	−0·2076	2·9692
8	0·7396	3·4509	+0·5200	2·9692
9	0·4503	3·7516	1·3446	2·9692
10	+0·1571	4·1890	2·2662	2·9692
11	−0·1246	4·7967	3·2848	2·9692
12	−0·3751	5·6121	+4·4005	2·9692

TABLE 8

Values of $\frac{K}{hV\alpha}$ *for Solutions* (a), (b), (c)

y'	Solution (a)	Solution (b)	Solution (c)
0	1·1257	1·1235	1·1319
1	1·1209	1·1187	1·1271
2	1·1064	1·1042	1·1127
3	1·0823	1·0799	1·0885
4	1·0484	1·0458	1·0546
5	1·0045	1·0017	1·0107
6	0·9501	0·9470	0·9564
7	0·8844	0·8808	0·8907
8	0·8051	0·8010	0·8112
9	0·7077	0·7031	0·7135
10	0·5830	0·5781	0·5880
11	0·4097	0·4053	0·4133
12	0	0	0

TABLE 9

Values of $\frac{C_{LL}c}{C_L\bar{c}} = \frac{7}{2} \cdot \frac{1}{C_L}\left(\frac{K}{hV}\right)$

$\eta = \frac{y'}{12}$	Vortex-lattice theory Ref. 2, solution 34	Method of present report, solution (c)
0	1·300	1·304
0·25	1·250	1·254
0·5	1·099	1·102
0·75	0·822	0·822
0·85	0·651	0·643
0·95	0·385	0·365

APPENDIX

Numerical Formula for J_3.

In order to determine numerical values of w_1/V in equation (39), it is required to evaluate

$$J_3 = \int_{-1}^{1}\int_{-1}^{1}\left(\xi\frac{\partial G}{\partial \xi} + \eta\frac{\partial G}{\partial \eta}\right)\frac{d\xi\, d\eta}{(\xi^2 + 4\eta^2)^{3/2}}$$

in terms of the values of $G(\xi, \eta)$, when $|\xi|$, $|\eta| = 0, \frac{1}{2}, 1$. Consider first the polynomial representation of $G(\xi, \eta)$ as a function of ξ only; then

$$G(\xi, \eta) = \tfrac{1}{3}a_{ij}G_j(\tfrac{1}{2}\xi)^i,$$

where the convention of suffix summation is used for $i, j = 0, 1, 2, 3, 4,$

$$G_j \text{ denotes } G\left(\frac{j-2}{2}, \eta\right)$$

and a_{ij} is given by the following table:

	$j = 0$	$j = 1$	$j = 2$	$j = 3$	$j = 4$
$i = 0$	0	0	+ 3	0	0
$i = 1$	+ 1	− 8	0	+ 8	− 1
$i = 2$	− 2	+ 32	− 60	+ 32	− 2
$i = 3$	−16	+ 32	0	− 32	+16
$i = 4$	+32	−128	+192	−128	+32

Similarly the polynomial representation in two variables is

$$G(\xi, \eta) = \tfrac{1}{9}a_{ij}a_{kl}G_{jl}(\tfrac{1}{2}\xi)^i(\tfrac{1}{2}\eta)^k,$$

where $$G_{jl} = G\left(\frac{j-2}{2}, \frac{l-2}{2}\right).$$

Therefore, the coefficient of $\xi^i\eta^k$ is

$$\tfrac{1}{9}(\tfrac{1}{2})^{i+k}a_{ij}a_{kl}G_{jl} = \tfrac{1}{9}(\tfrac{1}{2})^{i+k}A_{ik}\text{, say.}$$

Since $$\int_{-1}^{1}\int_{-1}^{1}\left(\xi\frac{\partial G}{\partial \xi} + \eta\frac{\partial G}{\partial \eta}\right)\frac{d\xi\, d\eta}{(\xi^2 + 4\eta^2)^{3/2}}$$

vanishes if $G(\xi, \eta)$ is odd in either ξ or η, it is only necessary to consider the coefficients A_{20}, A_{40}, A_{02}, A_{22}, A_{42}, A_{04}, A_{24}, A_{44}. Thus

$$J_3 = \tfrac{1}{9}\Sigma\,(\tfrac{1}{2})^{i+k}(i+k)A_{ik}I_{ik},$$

where $$I_{ik} = \int_{-1}^{1}\int_{-1}^{1}\frac{\xi^i\eta^k\, d\xi\, d\eta}{(\xi^2 + 4\eta^2)^{3/2}}$$

and (i, k) takes the 8 pairs of values. Now

$$I_{20} = \left[\left\{\eta\log_e\{\xi + \sqrt{(\xi^2 + 4\eta^2)}\}\right\}_{-1}^{1}\right]_{-1}^{1} = 2\log_e\frac{\sqrt{5}+1}{\sqrt{5}-1}$$

$$= 1\cdot92484730,$$

$$I_{40} = \left[\left\{- 2\eta^3 \log_e \{\xi + \surd(\xi^2 + 4\eta^2)\} + \tfrac{1}{2}\xi\eta\surd(\xi^2 + 4\eta^2)\right\}_{-1}^{1}\right]_{-1}^{1}$$

$$= - 4 \log_e \frac{\surd 5 + 1}{\surd 5 - 1} + 2\surd 5$$

$$= 0\cdot 62244136 ,$$

$$I_{02} = \left[\left\{ \tfrac{1}{8}\xi \log_e \{\surd(\xi^2 + 4\eta^2) + 2\eta\}\right\}_{-1}^{1}\right]_{-1}^{1} = \tfrac{1}{4} \log_e \frac{\surd 5 + 2}{\surd 5 - 2}$$

$$= 0\cdot 72181774 ,$$

$$I_{22} = \Big[\Big\{ \tfrac{1}{24}\, \xi^3 \log_e \{\surd(\xi^2 + 4\eta^2) + 2\eta\} + \tfrac{1}{3}\eta^3 \log_e \{\xi + \surd(\xi^2 + 4\eta^2)\}$$

$$- \tfrac{1}{12}\xi\eta\surd(\xi^2 + 4\eta^2)\Big\}_{-1}^{1}\Big]_{-1}^{1} = \tfrac{1}{12} \log_e \frac{\surd 5 + 2}{\surd 5 - 2} + \tfrac{2}{3} \log_e \frac{\surd 5 + 1}{\surd 5 - 1} - \tfrac{1}{3}\surd 5$$

$$= 0\cdot 13686568 ,$$

$$I_{42} = \Big[\Big\{ \tfrac{1}{40}\xi^5 \log_e \{\surd(\xi^2 + 4\eta^2) + 2\eta\} - \tfrac{6}{5}\eta^5 \log_e \{\xi + \surd(\xi^2 + 4\eta^2)\}$$

$$+ \tfrac{1}{20}\xi\eta\,(6\eta^2 - \xi^2)\surd(\xi^2 + 4\eta^2)\Big\}_{-1}^{1}\Big]_{-1}^{1}$$

$$= \tfrac{1}{20} \log_e \frac{\surd 5 + 2}{\surd 5 - 2} - \tfrac{12}{5} \log_e \frac{\surd 5 + 1}{\surd 5 - 1} + \surd 5$$

$$= 0\cdot 070614767 ,$$

$$I_{04} = \left[\left\{ - \tfrac{1}{64}\xi^3 \log_e\{\surd(\xi^2 + 4\eta^2) + 2\eta\} + \tfrac{1}{32}(\xi\eta\surd\xi^2 + 4\eta^2) \right\}_{-1}^{1}\right]_{-1}^{1}$$

$$= - \tfrac{1}{32} \log_e \frac{\surd 5 + 2}{\surd 5 - 2} + \tfrac{1}{8}\surd 5$$

$$= 0\cdot 18928128 ,$$

$$I_{24} = \Big[\Big\{ - \tfrac{3}{320}\xi^5 \log_e \{\surd(\xi^2 + 4\eta^2) + 2\eta\} + \tfrac{1}{5}\eta^5 \log_e \{\xi + \surd(\xi^2 + 4\eta^2)\}$$

$$+ \tfrac{1}{160}\,(3\xi^2 - 8\eta^2)\surd(\xi^2 + 4\eta^2)\Big\}_{-1}^{1}\Big]_{-1}^{1}$$

$$= - \tfrac{3}{160} \log_e \frac{\surd 5 + 2}{\surd 5 - 2} + \tfrac{2}{5} \log_e \frac{\surd 5 + 1}{\surd 5 - 1} - \tfrac{1}{8}\surd 5$$

$$= 0\cdot 051324632 ,$$

$$I_{44} = \Big[\Big\{ - \tfrac{3}{448}\xi^7 \log_e \{\surd(\xi^2 + 4\eta^2) + 2\eta\} - \tfrac{6}{7}\eta^7 \log_e \{\xi + \surd(\xi^2 + 4\eta^2)\}$$

$$+ \tfrac{1}{224}\xi\eta(3\xi^4 - 8\xi^2\eta^2 + 48\eta^4)\surd(\xi^2 + 4\eta^2) \Big\}_{-1}^{1}\Big]_{-1}^{1}$$

$$= - \tfrac{3}{224} \log_e \frac{\surd 5 + 2}{\surd 5 - 2} - \tfrac{12}{7} \log_e \frac{\surd 5 + 1}{\surd 5 - 1} + \tfrac{43}{56}\surd 5$$

$$= 0\cdot 02844285 .$$

Therefore, $J_3 = \frac{1}{9}\,[B_{20}I_{20} + B_{40}I_{40} + B_{02}I_{02} + B_{22}I_{22} + B_{42}I_{42} + B_{04}I_{04} + B_{24}I_{24} + B_{44}I_{44}]$,

where $B_{ik} = (\frac{1}{2})^{i+k}\,(i + k)A_{ik} = (\frac{1}{2})^{i+k}\,(i + k)a_{ij}a_{kl}G_{jl}$.

It follows from the table of a_{ij} that B_{ik} is given by the respective columns below:—

Factor of	B_{20}	B_{40}	B_{02}	B_{22}	B_{42}	B_{04}	B_{24}	B_{44}
G_{22}	−90	+144	−90	+900	−1080	+144	−1080	+1152
$G_{12} + G_{32}$	+48	− 96	0	−480	+ 720	0	+ 576	− 768
$G_{02} + G_{42}$	− 3	+ 24	0	+ 30	− 180	0	− 36	+ 192
$G_{21} + G_{23}$	0	0	+48	−480	+ 576	− 96	+ 720	− 768
$G_{11} + G_{13} + G_{31} + G_{33}$	0	0	0	+256	− 384	0	− 384	+ 512
$G_{01} + G_{03} + G_{41} + G_{43}$	0	0	0	− 16	+ 96	0	+ 24	− 128
$G_{20} + G_{24}$	0	0	− 3	+ 30	− 36	+ 24	− 180	+ 192
$G_{10} + G_{14} + G_{30} + G_{34}$	0	0	0	− 16	+ 24	0	+ 96	− 128
$G_{00} + G_{04} + G_{40} + G_{44}$	0	0	0	+ 1	− 6	0	− 6	+ 32

Hence,

$$\begin{aligned} J_3 = &- 10{\cdot}7845628\,\{G(0, 0)\} + 2{\cdot}8338092\,\{G(-\tfrac{1}{2}, 0) + G(\tfrac{1}{2}, 0)\} \\ &+ 0{\cdot}4636337\,\{G(-1, 0) + G(1, 0)\} + 0{\cdot}7293835\,\{G(0, -\tfrac{1}{2}) + G(0, \tfrac{1}{2})\} \\ &+ 0{\cdot}3084028\,\{G(-\tfrac{1}{2}, -\tfrac{1}{2}) + G(-\tfrac{1}{2}, \tfrac{1}{2}) + G(\tfrac{1}{2}, -\tfrac{1}{2}) + G(\tfrac{1}{2}, \tfrac{1}{2})\} \\ &+ 0{\cdot}2422526\,\{G(-1, -\tfrac{1}{2}) + G(-1, \tfrac{1}{2}) + G(1, -\tfrac{1}{2}) + G(1, \tfrac{1}{2})\} \\ &+ 0{\cdot}0181922\,\{G(0, -1) + G(0, 1)\} \\ &+ 0{\cdot}0879315\,\{G(-\tfrac{1}{2}, -1) + G(-\tfrac{1}{2}, 1) + G(\tfrac{1}{2}, -1) + G(\tfrac{1}{2}, 1)\} \\ &+ 0{\cdot}0350445\,\{G(-1, -1) + G-(1, 1) + G(1, -1) + G(1, 1)\}\,. \end{aligned}$$

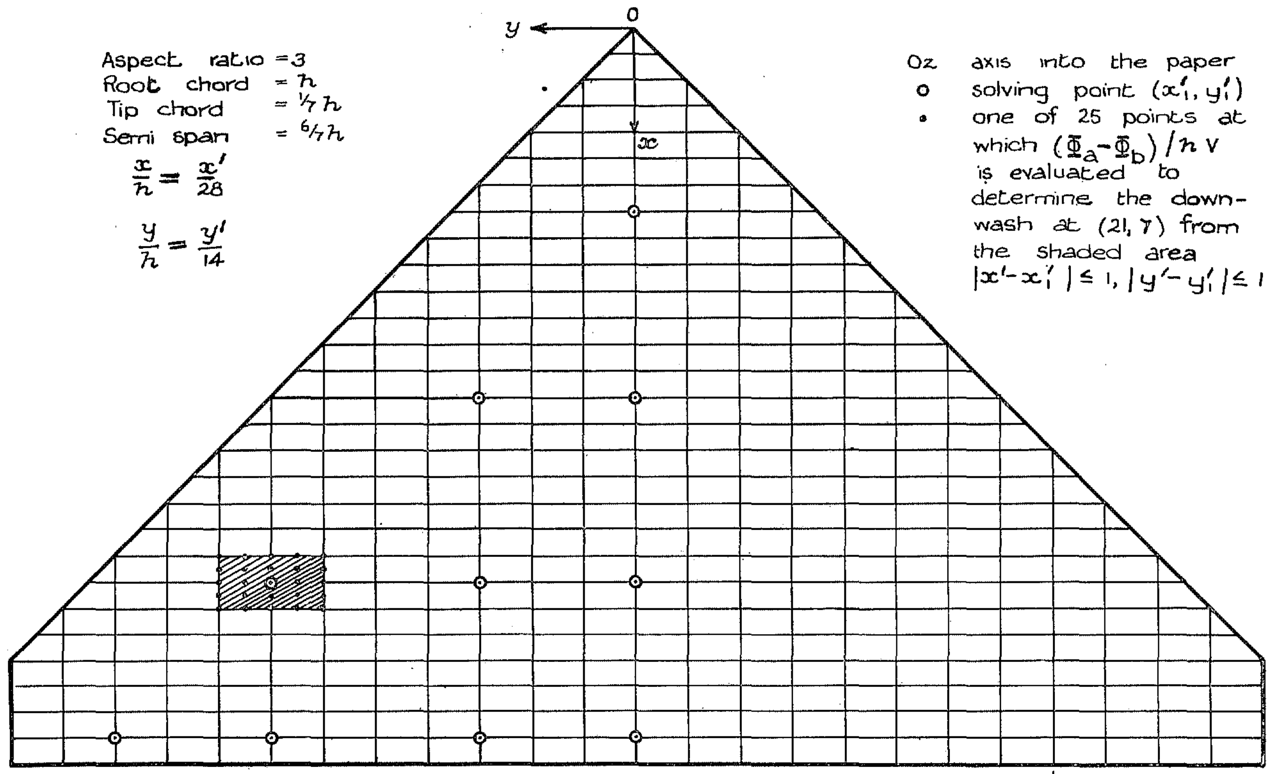

FIG. 1. Plan form of the delta wing.

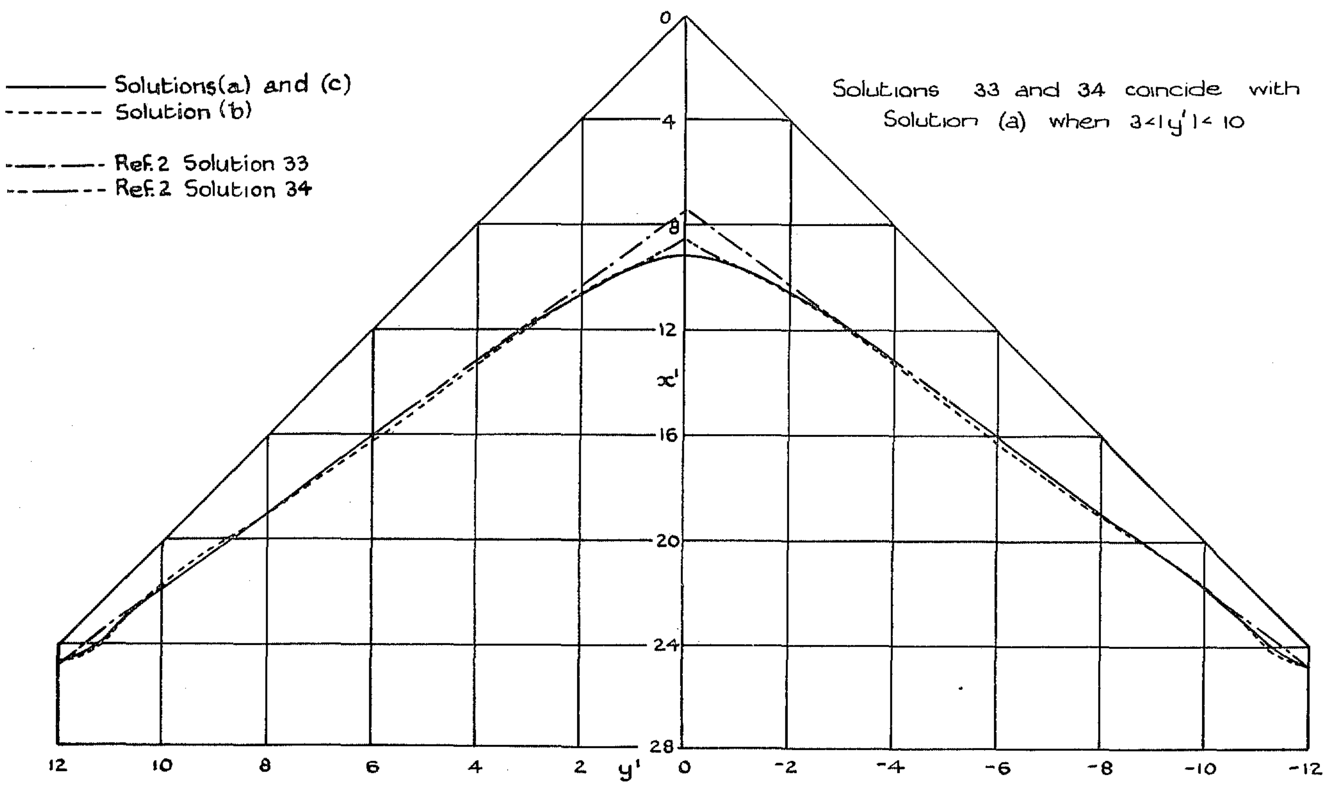

FIG. 2. Loci of the chordwise centres of pressure along sections of the delta wing.

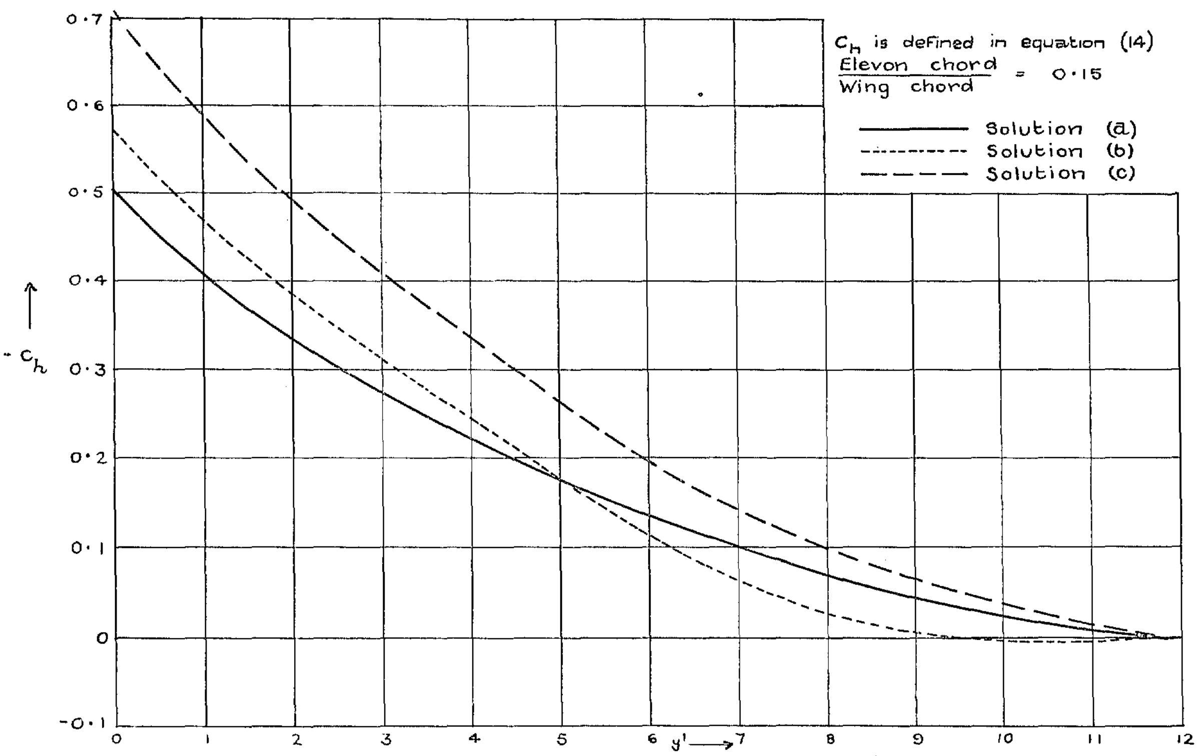

FIG. 3. Spanwise distribution of hinge moment on the undeflected elevon.

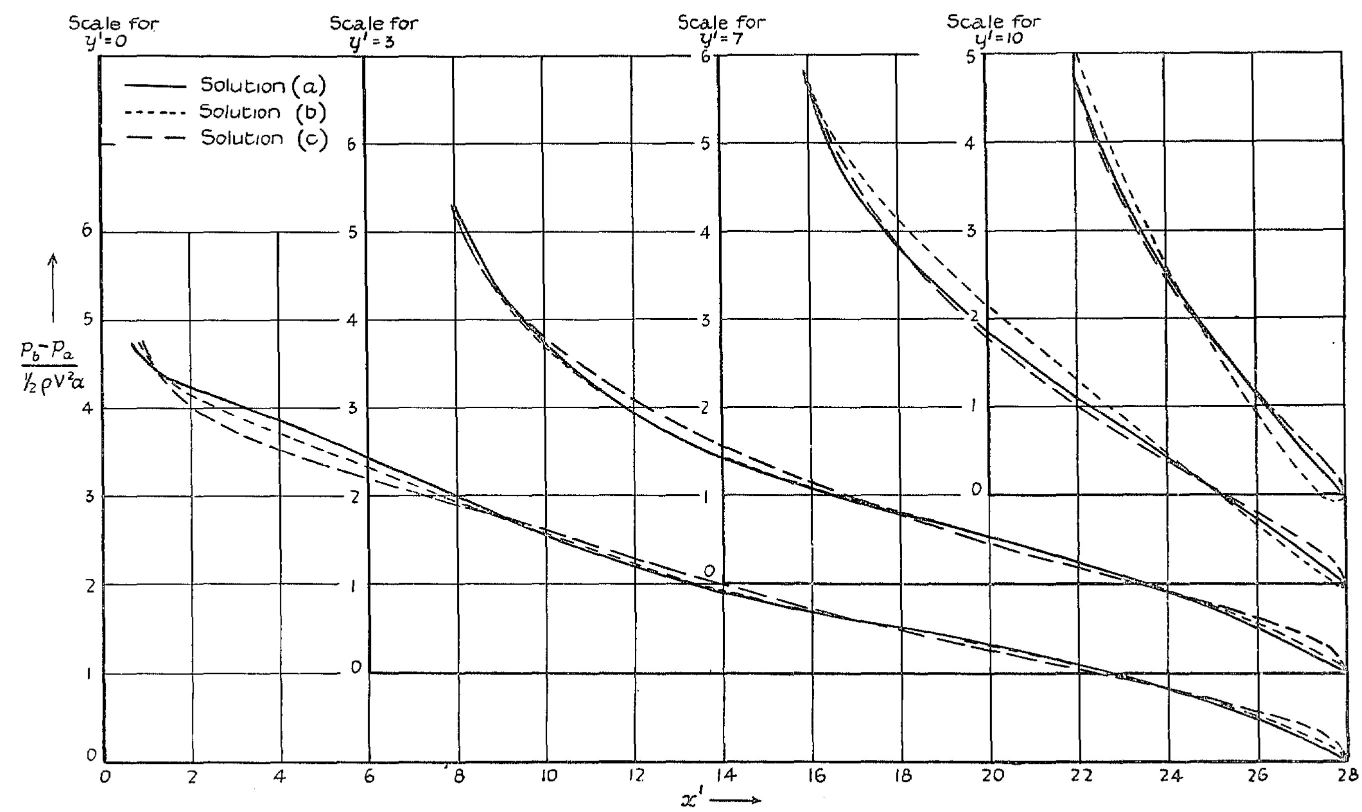

FIG. 4. Distributions of pressure difference along four sections of the delta wing.

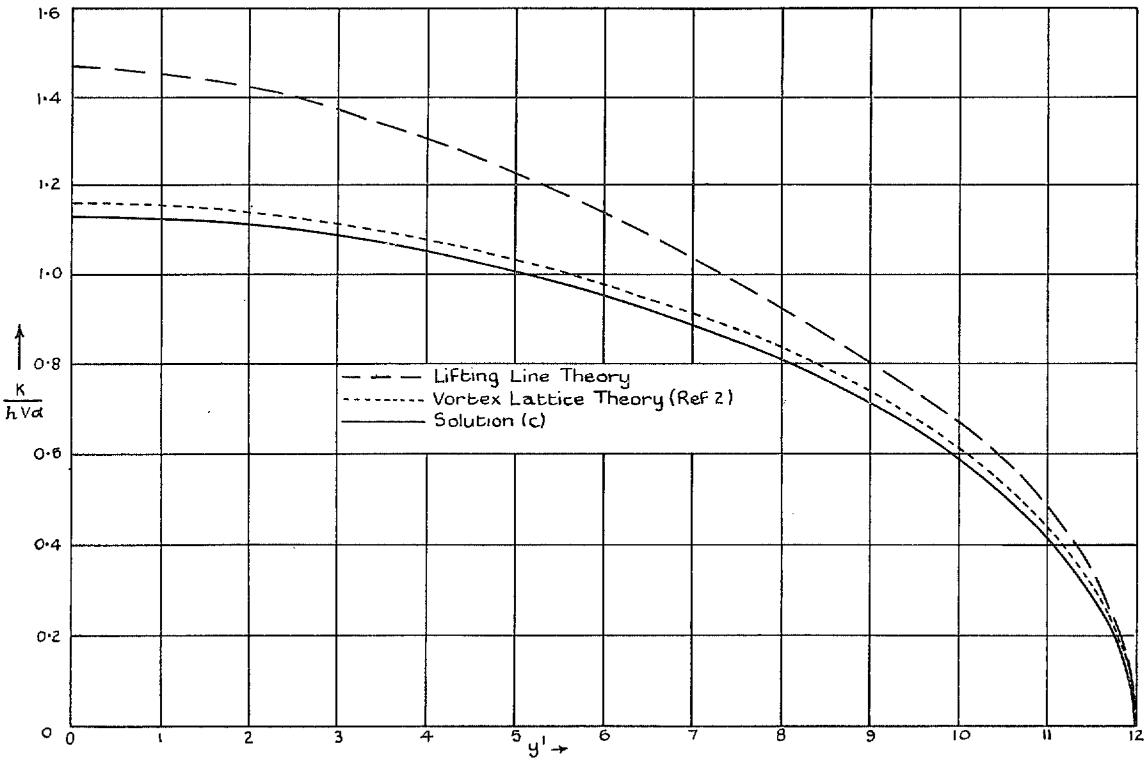

FIG. 5. Comparison of spanwise distributions of circulation round the delta wing.

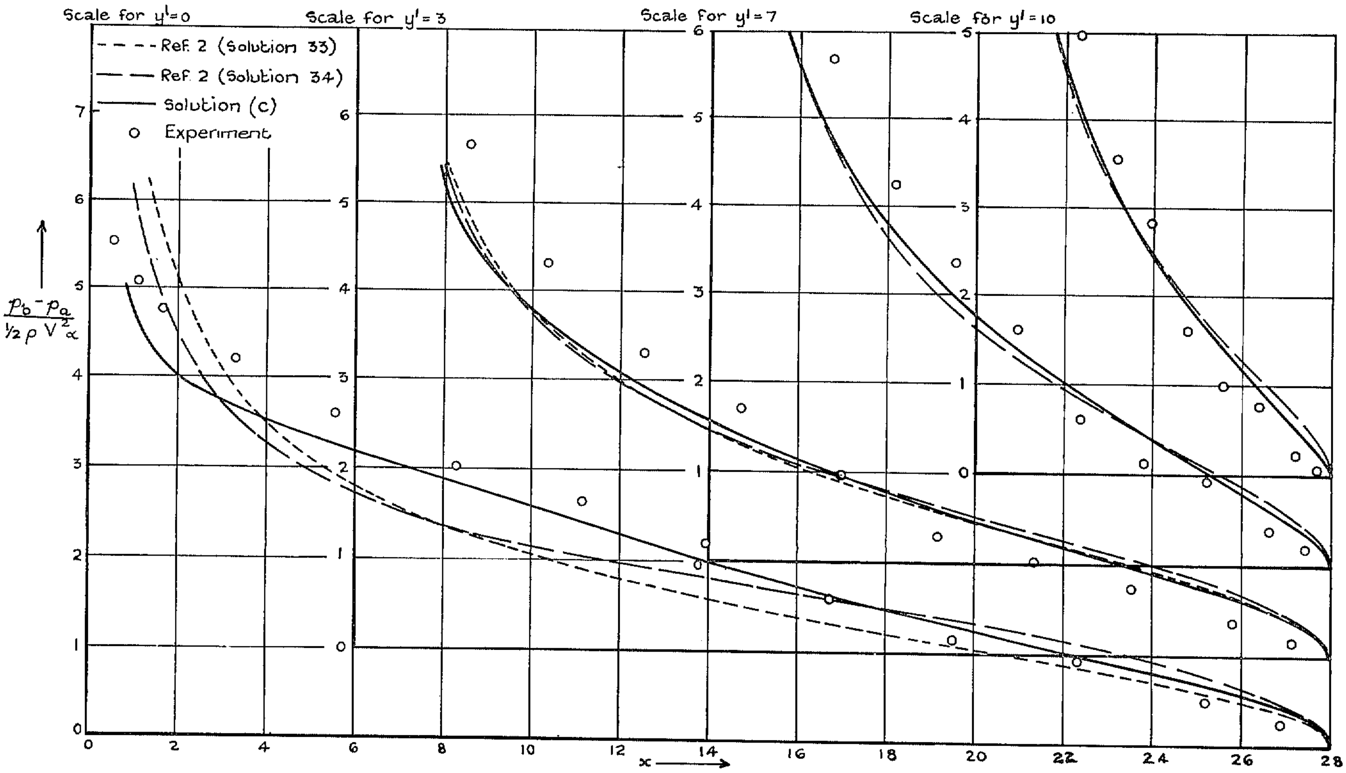

FIG. 6. Comparison of pressure distributions from solution (c), vortex-lattice theory and experiment.

(59008) Wt. 17/680 K.9 9/54 Hw.

PRINTED IN GREAT BRITAIN

Publications of the Aeronautical Research Council

ANNUAL TECHNICAL REPORTS OF THE AERONAUTICAL RESEARCH COUNCIL (BOUND VOLUMES)

1936 Vol. I. Aerodynamics General, Performance, Airscrews, Flutter and Spinning. 40*s.* (41*s.* 1*d.*)
Vol. II. Stability and Control, Structures, Seaplanes, Engines, etc. 50*s.* (51*s.* 1*d.*)

1937 Vol. I. Aerodynamics General, Performance, Airscrews, Flutter and Spinning. 40*s.* (41*s.* 1*d.*)
Vol. II. Stability and Control, Structures, Seaplanes, Engines, etc. 60*s.* (61*s.* 1*d.*)

1938 Vol. I. Aerodynamics General, Performance, Airscrews. 50*s.* (51*s.* 1*d.*)
Vol. II. Stability and Control, Flutter, Structures, Seaplanes, Wind Tunnels, Materials. 30*s.* (31*s.* 1*d.*)

1939 Vol. I. Aerodynamics General, Performance, Airscrews, Engines. 50*s.* (51*s.* 1*d.*)
Vol. II. Stability and Control, Flutter and Vibration, Instruments, Structures, Seaplanes, etc. 63*s.* (64*s.* 2*d.*)

1940 Aero and Hydrodynamics, Aerofoils, Airscrews, Engines, Flutter, Icing, Stability and Control, Structures, and a miscellaneous section. 50*s.* (51*s.* 1*d.*)

1941 Aero and Hydrodynamics, Aerofoils, Airscrews, Engines, Flutter, Stability and Control, Structures. 63*s.* (64*s.* 2*d.*)

1942 Vol. I. Aero and Hydrodynamics, Aerofoils, Airscrews, Engines. 75*s.* (76*s.* 3*d.*)
Vol. II. Noise, Parachutes, Stability and Control, Structures, Vibration, Wind Tunnels. 47*s.* 6*d.* (48*s.* 7*d.*)

1943 Vol. I. Aerodynamics, Aerofoils, Airscrews. 80*s.* (81*s.* 4*d.*)
Vol. II. Engines, Flutter, Materials, Parachutes, Performance, Stability and Control, Structures. 90*s.* (91*s.* 6*d.*)

1944 Vol. I. Aero and Hydrodynamics, Aerofoils, Aircraft, Airscrews, Controls. 84*s.* (85*s.* 8*d.*)
Vol. II. Flutter and Vibration, Materials, Miscellaneous, Navigation, Parachutes, Performance, Plates and Panels, Stability, Structures, Test Equipment, Wind Tunnels. 84*s.* (85*s.* 8*d.*)

Annual Reports of the Aeronautical Research Council—

1933–34	1*s.* 6*d.* (1*s.* 8*d.*)	1937	2*s.* (2*s.* 2*d.*)
1934–35	1*s.* 6*d.* (1*s.* 8*d.*)	1938	1*s.* 6*d.* (1*s.* 8*d.*)
April 1, 1935 to Dec. 31, 1936	4*s.* (4*s.* 4*d.*)	1939–48	3*s.* (3*s.* 2*d.*)

Index to all Reports and Memoranda published in the Annual Technical Reports, and separately—

April, 1950 - - - - R. & M. No. 2600. 2*s.* 6*d.* (2*s.* 7½*d.*)

Author Index to all Reports and Memoranda of the Aeronautical Research Council—

1909–1949. R. & M. No. 2570. 15*s.* (15*s.* 3*d.*)

Indexes to the Technical Reports of the Aeronautical Research Council—

December 1, 1936 — June 30, 1939.	R. & M. No. 1850.	1*s.* 3*d.* (1*s.* 4½*d.*)
July 1, 1939 — June 30, 1945.	R. & M. No. 1950.	1*s.* (1*s.* 1½*d.*)
July 1, 1945 — June 30, 1946.	R. & M. No. 2050.	1*s.* (1*s.* 1½*d.*)
July 1, 1946 — December 31, 1946.	R. & M. No. 2150.	1*s.* 3*d.* (1*s.* 4½*d.*)
January 1, 1947 — June 30, 1947.	R. & M. No. 2250.	1*s.* 3*d.* (1*s.* 4½*d.*)
July, 1951.	R. & M. No. 2350.	1*s.* 9*d.* (1*s.* 10½*d.*)

Prices in brackets include postage.

Obtainable from

HER MAJESTY'S STATIONERY OFFICE

York House, Kingsway, London, W.C.2; 423 Oxford Street, London, W.1 (Post Orders: P.O. Box 569, London, S.E.1); 13a Castle Street, Edinburgh 2; 39, King Street, Manchester 2; 2 Edmund Street, Birmingham 3; 1 St. Andrew's Crescent, Cardiff; Tower Lane, Bristol 1; 80 Chichester Street, Belfast, or through any bookseller

S.O. Code No. 23-2819